

AD-R172 914

THE EFFECT OF IONIZING RADIATION ON THE BREAKDOWN

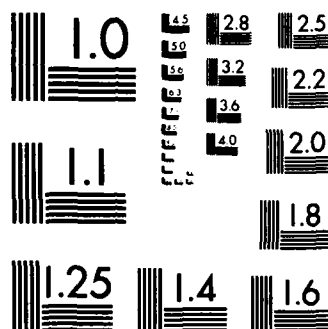
111

UNCLASSIFIED

AFIT/CI/NR-86-182T

F/G 9/1

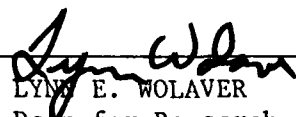
NL



MICROCOPY RESOLUTION TEST CHART
NATIONAL BUREAU OF STANDARDS-1963-A

REPORT DOCUMENTATION PAGE

READ INSTRUCTIONS
BEFORE COMPLETING FORM

1. REPORT NUMBER AFIT/CI/NR 86-182T		2. GOVT ACCESSION NO.	3. RECIPIENT'S CATALOG NUMBER
4. TITLE (and Subtitle) The Effect of Ionizing Radiation on the Breakdown Voltage of Power MOSFETs		5. TYPE OF REPORT & PERIOD COVERED THESIS/DISSERTATION	
		6. PERFORMING ORG. REPORT NUMBER	
7. AUTHOR(s) Robert Dale Pugh		8. CONTRACT OR GRANT NUMBER(s)	
9. PERFORMING ORGANIZATION NAME AND ADDRESS AFIT STUDENT AT: University of Washington		10. PROGRAM ELEMENT, PROJECT, TASK AREA & WORK UNIT NUMBERS	
11. CONTROLLING OFFICE NAME AND ADDRESS		12. REPORT DATE 1986	
		13. NUMBER OF PAGES 81	
14. MONITORING AGENCY NAME & ADDRESS (if different from Controlling Office)		15. SECURITY CLASS. (of this report) UNCLASS	
		15a. DECLASSIFICATION/DOWNGRADING SCHEDULE	
16. DISTRIBUTION STATEMENT (of this Report) APPROVED FOR PUBLIC RELEASE; DISTRIBUTION UNLIMITED			
17. DISTRIBUTION STATEMENT (of the abstract entered in Block 20, if different from Report)			
18. SUPPLEMENTARY NOTES APPROVED FOR PUBLIC RELEASE: IAW AFR 190-1		 LYNN E. WOLAVER Dean for Research and Professional Development AFIT/NR	
19. KEY WORDS (Continue on reverse side if necessary and identify by block number)			
20. ABSTRACT (Continue on reverse side if necessary and identify by block number) ATTACHED ...			

DTIC
OCT 15 1986
E

AD-A172 914

DTIC FILE COPY

The Effect of Ionizing Radiation on the Breakdown Voltage of
Power MOSFETs

by

ROBERT DALE PUGH

A thesis submitted in partial fulfillment
of the requirements for the degree of

Master of Science in Nuclear Engineering

University of Washington

1986

Approved by


(Chairperson of Supervisory Committee)

Program Authorized
to Offer Degree Department of Nuclear Engineering

Date August 13, 1986

In presenting this thesis in partial fulfillment of the requirements for a Master's degree at the University of Washington, I agree that the Library shall make its copies freely available for inspection. I further agree that extensive copying of this thesis is allowable only for scholarly purposes, consistent with "fair use" as prescribed in the U.S. Copyright Law. Any other reproduction for any purpose or by any means shall not be allowed without my written permission.

Signature Robert D. Ingham

Date August 13, 1986



Acceptance For	
10/15/86	<input checked="checked" type="checkbox"/>
10/15/86	<input type="checkbox"/>
10/15/86	<input type="checkbox"/>
A-1	

TABLE OF CONTENTS

	Page
Chapter 1: Introduction	1
Chapter 2: Summary and Conclusions	4
Conclusion	7
Chapter 3: Solid-State Physics	9
Semiconductors	9
P-N Junctions	12
Chapter 4: Field-Effect: Theory, Characteristics, and Design.	16
Characteristics of MOS Transistors.	17
Power MOSFET Design	19
Radiation Effects.	20
Threshold Voltage	21
Avalanche Breakdown	23
Chapter 5: Field Termination Techniques	28
Field Rings	29
Field Plates	32
Junction Termination Extension.	34
Chapter 6: Experimental Procedure	36
Typical Experimental Procedure	36
Experimental Procedure and Equipment.	37
The Controller Board.	39
The Computer	41
Auxiliary Tests	42
Testing the Equipment Set-up	42
Procedure Verification.	42
Baselining the FETs.	45
Optical Microscope and Microprobing.	46
Chapter 7: Results and Discussion	48
N-Channel Results	49
P-Channel Results	53
Chapter 8: Conclusions	58
References	61
Appendix A: COOLDOWN -- A Pascal Program to Evaluate MOSFET Breakdown Voltage	63
Appendix B: A Representative Data File	74

LIST OF FIGURES

Number	Page
1. Expected P-Channel Results	5
2. P-Channel Results Showing Decrease in V_{BD} at Low Dose	5
3. Results of P-Channel Device Showing Decrease with No Recovery. . .	6
4. N-Channel Result Showing Detail	6
5. N and P Type Materials Before and After Contact	13
6. Electric Field and Barrier Potential Across a Depletion Region of Width W	14
7. Double (N-P-N) Junction	17
8. N-P-N Junction with Conductor Above P-Type Material	18
9. N-P-N Junction with N-Channel	18
10. Schematic Diagram of VD MOSFET	20
11. Operation of a Power MOSFET.	20
12. Thermally Induced Ionization Effects	24
13. Example of a Plane P-N Junction	28
14. Example of a Curved P-N Junction	29
15. Example of a Field Ring Terminator	30
16. The Depletion Region Shape with No V_{DS} , Moderate V_{DS} , and After Punch-through	30
17. Breakdown Voltage of a Curved Junction With and Without Field Rings	31
18. Sensitivity of Field Ring Placement	32
19. Example of Field Plate Termination of a P-N Junction	33
20. Example of a Junction Termination Extension	35
21. Equipment Set-up	38
22. Schematic Diagram of Controller Circuit	40
23. Results of First Experiment Showing Noise	55
24. The Change in Breakdown Voltage During Gamma Irradiation	49
25. Breakdown Voltage Change with Increasing Dose in a 350V N-Channel	50
26. Breakdown Voltage of Two N-Channel FETs With Field Rings	51
27. Breakdown Voltage of a 500V N-Channel FET	52
28. Results of Irradiating a Very-High Voltage N-Channel Device.	53

29	Change in P-Channel Breakdown Voltage During Gamma Irradiation .	54
30	Change in P-Channel Breakdown Voltage During Gamma Irradiation .	54
31	Change in Breakdown Voltage of a Moderate Voltage P-Channel FET .	55
32	Results of Another Moderate Voltage P-Channel FET	56
33	Change in Breakdown Voltage for Low Voltage P-Channel MOSFET. . .	57

LIST OF TABLES

Number	Page
1. Characteristics of Devices Tested	48

ACKNOWLEDGMENTS

I am happy to have this opportunity to thank the many people and organizations who have made this research project possible. First, I would like to thank the companies who provided the FETs I used in my experiments: Pacific Electro Dynamics of Redmond, Washington and Supertex Inc. of Sunnyvale, California. I would like to thank my contacts in those organizations, Stan Patterson and Chuck Koehler respectively, for providing me with FETs which yielded interesting information. I also want to thank the U.S. Air Force for taking a chance and supporting me through both my undergraduate and graduate study programs. I will do my best to show them they made a sound choice.

Two other organizations played a significant role in this research: the Boeing Radiation Effects Laboratory (BREL) and the university of Washington Nuclear Engineering Department. Without the use of the facilities at BREL, an experiment like the one I performed would have been nearly impossible. I am also indebted to the BREL staff. Although a list of BREL staff members who helped me would be too large for the space I have here, I would like to acknowledge Itsu Aurimura, Mark Baze, Rick Kennerud, and Wes Will for always being willing to work with me on both the technical and theoretical problems I had.

The faculty and staff of the Nuclear Engineering Department have been an inspiration to me throughout my time here; I never expected such an open-minded tolerance of my maverick ideas. I do believe, though, that we all benefited from it. I would like to single out the members of my thesis committee, Drs. Babb, Garlid, and Rowe, as well as Dr. McCormick for the guidance and encouragement they have provided.

I wish I could find a way to properly thank the two men who conceived of and directed my research. In the way of a compliment, I want to say I think both of these men are true scientists. Dr. Ken Galloway of the National bureau of

Standards and the University of Maryland originally proposed the topic of my research and provided a lot of sound technical guidance and encouragement. Allan Johnston of BREL is the other member of my technical team. I owe Allan a debt I will never be able to repay. He agreed to work with me on this project without any idea of what the outcome would be. Throughout the course of the work, he guided the direction of my research and helped me develop my understanding of the underlying electrical engineering and solid-state physics concepts which I was not familiar with. Through the last eight months, Allan spent many hours of his own time counseling, tutoring, discussing the direction of the research, analyzing the data, and interpreting the results. His only reward is a somewhat increased understanding of power devices, a second authorship on the paper we wrote, and my thanks. Allan, I thank you and I want to say I am honored to know you.

Finally, I want to thank my entire family for the support and encouragement they have given to me. I really want to thank my children for the way they have tolerated my short temper in stressful times and my absence the rest of the time these last few years. Last, and most of all, I want to thank my wife Elaine. For the past four years I have been on sabbatical from my family responsibilities. She "picked up the slack" and did the things I should have done so that I could pursue my higher education. As a small token of the appreciation I have for her contributions, I dedicate this work in her honor. Elaine, thank you for everything.

CHAPTER 1

INTRODUCTION

Vertical double-diffused (VD) metal-oxide-semiconductor (MOS) field-effect-transistor (FET), or VD MOSFET, is an awkward, intimidating name, but it succinctly describes the structure and operation of a very useful solid state device. First developed in the early 1980s, VD MOSFETs (also called power MOSFETs) have become widely used in the electronic industry due to their ability to switch large currents at high frequencies (10-100 kHz) and because of their thermal ruggedness.¹ VD MOSFETs are particularly useful in both space and military applications because they allow engineers to design power supplies that work at high frequencies; with higher power supply frequencies the size of the transformers, and therefore the weight of the systems, can be reduced significantly.

Space-based systems operate in a cosmic radiation environment, and military radiation-hardness specifications must be satisfied; therefore, the effect of radiation on the operating characteristics of devices to be used in either application must be well known. The MOSFET structure is resistant to neutron damage at normally encountered fluences; however, they are sensitive to gamma radiation. Designers are primarily interested in knowing the effect of gamma radiation on the threshold voltage (V_{TH}) and breakdown voltage (V_{BD}) of MOSFETs. These two parameters are very important because, if they change, the behavior of a MOSFET in a circuit can change drastically. 4

As a crude analogy, a MOSFET can be considered the electrical counterpart of an electrically controlled gate valve. It is reasonable to assume that applying some small voltage to the gate accomplishes nothing. At a gate voltage above some cut-off level (V_{TH}), the valve begins to open slightly. At gate voltages above the cut-off level, increasing the gate voltage opens the valve farther and increases the flow through the valve up to a point. Above some level of gate voltage, the gate is completely open and flow has achieved a maximum value. Increasing the gate voltage beyond this point

causes no change in the flow through the valve. In the case of a MOSFET, the flow through the valve corresponds to the electrical current which flows through the MOSFET.

In order to "model" the breakdown voltage, we must assume that this valve has some maximum pressure that it can withstand. At pressures exceeding this maximum, the gate of the valve will fail, allowing an unrestricted flow through the valve. The MOSFET analog of the pressure against the gate is the drain-source voltage (the drain and source are the input and output of a MOSFET) and the maximum pressure the valve can withstand corresponds to V_{BD} .

It is now easy to see how a change in V_{TH} or V_{BD} can change the performance of a circuit. If V_{TH} decreases, the MOSFET may turn on sooner than it is supposed to. In some cases, V_{TH} can decrease to the point where the MOSFET is always turned on. Another possibility is that V_{TH} increases. If so, it is possible that the MOSFET will not turn on when signaled to do so. An increase in V_{BD} will have a negligible effect on the operation of the MOSFET. A decrease in V_{BD} , however, can have catastrophic results. Frequently, MOSFETs are used to switch the current in a circuit on and off. If V_{BD} decreases below the applied drain-source voltage, the MOSFET will not be able to turn the current off.

Past research has attempted to identify how gamma radiation affects the breakdown voltage and the threshold voltage of VD MOSFETs in general.²⁻⁵ Although there have been many models proposed to predict the results of irradiating specific FETs,²⁻⁵ it has been shown that small manufacturing differences of two similar FETs can cause a significant difference in the effect of radiation on the devices.⁶ These complications have defeated the attempts to develop a general analytical model.

There has been a lot of earlier research on the effects of gamma radiation on threshold voltage of power MOSFETs,^{2,3} but only recently have researchers begun to look at the effect of radiation on breakdown voltage.^{7,8} In 1983 Joseph Benedetto at the University of Maryland proposed a way of

predicting the trend in the radiation induced change in V_{BD} for n-channel VD MOSFETs.⁷ His model was based on the type of electric field termination used in the device (these terms will be explained in Chapter 1). Using the results from experiments he performed on power MOSFETs, Benedetto proposed that, in general, V_{BD} decreased in n-channel FETs with increasing dose. Depending on the type of termination technique employed by the manufacturer though, he found with some types of terminations there was a partial recovery toward the initial breakdown voltage as the dose increased beyond some value. One of Benedetto's auxiliary proposals was that the breakdown voltage for high-voltage p-channel MOSFETs could be expected to increase during irradiation rather than decrease as do n-channel MOSFETs.

The original purpose of this research was to verify Benedetto's proposed model of gamma-radiation-induced breakdown voltage changes in p-channel MOSFETs by experimentation. Early experimentation, however, indicated that Benedetto's modeling concepts were too simple and could not account for some of the experimental results. The purpose was then expanded to include investigating the role of field termination designs, as well as other characteristics which affect radiation-induced breakdown voltage changes.

The results presented in this thesis show that ionizing radiation can cause substantial changes in the breakdown voltage of power MOSFETs. The magnitude and direction (sign) of the breakdown voltage change can be related to the type of termination technique which is used and how well the termination is optimized. This thesis also relates these results to a general theory of termination techniques, and explains why large changes in breakdown voltage are expected for only high breakdown voltage devices, a finding which is consistent with the observed results of the experiments.

CHAPTER 2

SUMMARY AND CONCLUSIONS

The initial purpose of this research was to verify that the breakdown voltage of p-channel MOSFETs increased as a result of exposure to ionizing radiation as had been proposed by Benedetto. Additionally, termination theory was studied in order to understand how the effectiveness of electric field terminations is changed by ionizing radiation. This study was included because early experiments revealed some shortcomings in Benedetto's proposed model and since earlier experiments, including Benedetto's, indicated a link between the type of electric field terminations used in a device and the radiation-induced change in V_{BD} .

To investigate the radiation induced changes, my advisor, Allan Johnston of the Boeing Radiation Effects Laboratory (BREL), and myself devised a test procedure that allowed us to measure the breakdown voltage of MOSFETs during irradiation (*in-situ*) in a gamma radiation test fixture (gamma cell). This procedure measured the breakdown voltage much more frequently than had usually been done in earlier experiments.⁷ In order to gather a large number of data points during each experiment (125 per hour), the experiments were run by a computer. An optical microscope was used to identify the termination techniques used in the MOSFETs tested in the experiments. Additionally, a microscope and microprobes were used to determine if the termination devices were internally connected to either the gate or the source of the device. This was important in order to be able to determine what voltage was applied to the termination devices during irradiation.

The results of the p-channel experiments did not agree with the models proposed by Benedetto. Specifically, the results revealed that V_{BD} of some p-channel MOSFETs increased with irradiation as was anticipated by the proposed model (see Figure 1). In several types of p-channel devices, however, V_{BD} consistently decreased and then recovered (see Figure 2). Furthermore, the breakdown voltage of one type of p-channel device

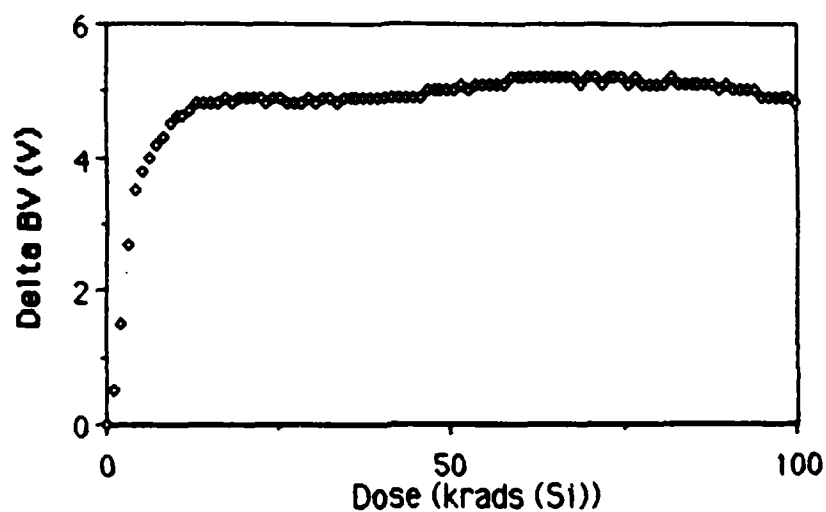


Figure 1: Expected P-Channel Results

decreased by about a factor of two and remained low at higher dose levels (see Figure 3), in sharp contrast to the predictions. From these figures it is easy to identify the difference between the expected and observed results.

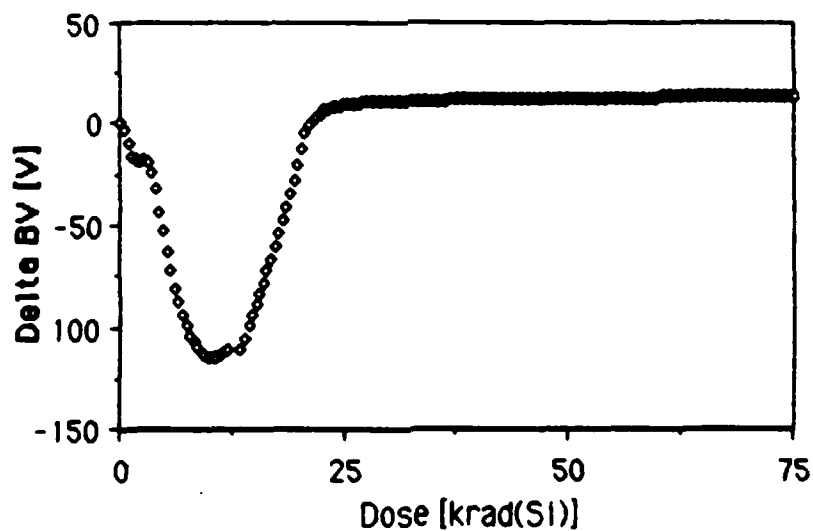


Figure 2: P-Channel Results Showing Decrease in V_{BD} at Low Dose

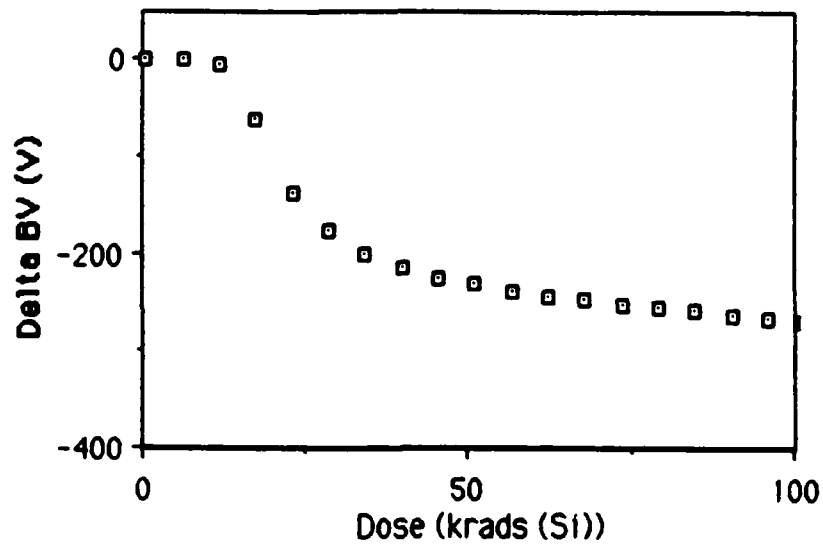


Figure 3: Results of P-Channel Device Showing Decrease with No Recovery

Several n-channel devices were also tested. Although, in general, the results were in agreement with Benedetto's experiments, the increased number of data points taken revealed some detail in the plots of V_{BD} versus dose that had not been observed earlier (see Figure 4).

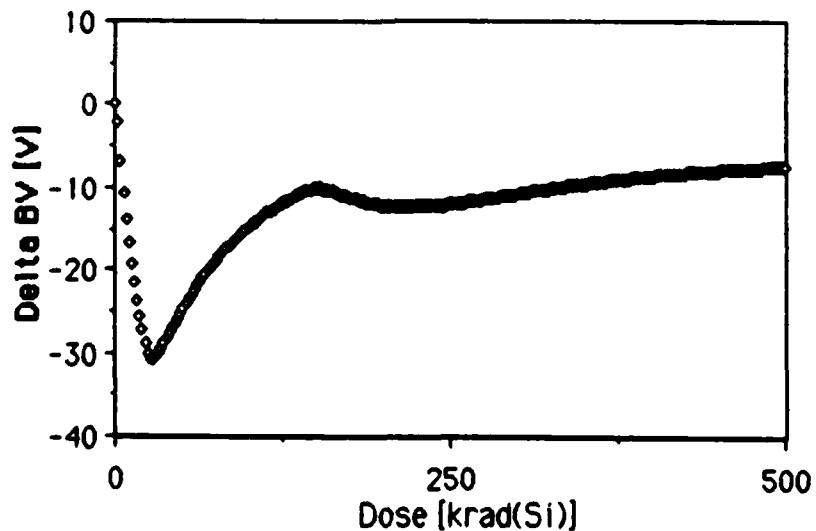


Figure 4: N-Channel Result Showing Detail

Further investigation indicated that many device manufacturers use combinations of more than one termination type. This process complicates attempts to predict the effect of radiation on a particular device, and explains why the results could not be consistently predicted by simple models. Research into published material revealed that other device characteristics like oxide thickness and oxide purity also effect the radiation induced changes in device performance.⁹

Conclusions

This research has shown that different types of MOSFETs, even if they have similar internal structure, can exhibit different radiation-induced changes in breakdown voltage which could render the MOSFET inoperative. The first difference, which is not surprising, is that n-channel and p-channel MOSFETs generally react differently to ionizing radiation. Another difference, which had been proposed by Benedetto, is that the type of field termination technique used in a device has a direct bearing on the magnitude and direction of the change.

One finding that had not been provided in a single source form before was an analysis of the general theory of the commonly used electric field termination device types. This theory predicts quite accurately the effect of radiation on the breakdown voltage in "well behaved" devices. By "well behaved", I mean devices which use field plates or junction termination extensions and have pure field oxides of a known thickness. In the case of field rings the effect is not so easy to predict since how optimally the rings have been positioned plays the dominant role in determining the response to radiation.

The most important finding of this project is that other device characteristics, such as oxide purity and oxide thickness, which can vary from unit to unit in the same model of FET, can affect the response of transistors. These individualized peculiarities, along with the use of more than one termination type in a type of FET and the casual attitude that manufacturers have about changing termination techniques without notifying circuit designers, makes it extremely difficult to develop a general model for

the radiation induced change in V_{BD} .

This potential variation between units indicates that it is essential to use an experimental procedure which makes "continuous" measurements of V_{BD} , preferably during irradiation, when attempting to determine the response of a type of FET to ionizing radiation. This is because results which are obtained by averaging together data from several units which was obtained at widely separated, discrete doses can mask the details which are needed to make an accurate determination. A "continuous" measurement procedure was developed as a part of this research.

CHAPTER 3

SOLID-STATE PHYSICS

Before discussing the research project further, I will briefly review the underlying solid-state physics that govern the operation of contemporary solid-state devices. Those who are interested in further reading on the subject, can find a thorough explanation in most introductory electronic device texts, for example Physics and Technology of Semiconductor Devices (ref 10) or Transistors (ref 11).

Semiconductors

When thinking of modern solid-state electronic devices, one usually imagines things like micro chips containing complex integrated circuits. Equally remarkable advances have also been made in discrete components, particularly power devices, which are at the opposite ends of the solid-state spectrum. Diodes, transistors, and thyristors are available which can hold off potentials of thousands of volts across a junction much less than a 100 μm (micrometers) thick. The operation of all these devices is based on the electrical characteristics of a chemically treated (doped) crystal of silicon or germanium: elements from column IV in the periodic table.[†] The following discussion is based on a device constructed out of silicon; however, a similar discussion would apply to any elements used in semiconductor fabrication.

Solids can be divided into three classes: insulators, semiconductors, and conductors. The band theory of solids uses quantum mechanical arguments to show that the allowed energy states of electrons in a periodic array (lattice) of atoms occur in groups (bands) of energy levels.*

[†] There are also several compounds like Gallium arsenide (GaAs) which are used to manufacture some solid-state devices but are not used for power devices.

* An elegant treatment of the quantum-mechanical explanation of energy bands is included in Transistors, section 2-2.2.

Within a given band, the allowed electron energies are closely spaced, but there can be large differences (gaps) between the highest allowed energy of one band and the lowest energy of the next.

At very low temperatures (near absolute zero), the electrons are in their lowest energy state and are all in the lowest band which is called the valence band. As the temperature is increased, it is possible for some of the electrons to be excited (jump) into the next band which is called the conduction band. The distance between these two bands is called the forbidden gap and corresponds to the amount of energy that must be given to an electron to boost it into the next band (ionize the atom). The width of the forbidden band is what determines the difference between insulators, semiconductors, and conductors.

In a conductor (metal) the valence and conduction bands overlap so that the electrons are easily moved into the conduction band. This means that electrons in a metal are free to move if even a small electric field is applied. As you might expect, this is not the case with insulators. Since the valence electrons in an insulator form strong valence bonds with their neighbors, the valence and conduction bands in an insulator are far apart. For this reason, it is difficult to impart sufficient energy to an electron of an insulator to jump the gap into the conduction band.

Semiconductors, as the name implies, fall somewhere in between conductors and insulators. The valence and conduction bands in a semiconductor are close enough together that an electron only needs a moderate amount of energy to jump into the conduction band. This is because in a silicon crystal, each atom in the lattice shares one valence electron with each of its four neighbors. These bonds are only moderately strong and can be broken by molecular vibration at fairly low temperatures (ionization).

Once a bond is broken, the resulting (free) electron in the conduction band will move if an electric potential is applied across the crystal. The absence of the electron from the valence band creates a vacancy which is called a "hole". A "hole" is a construct which is used to help visualize the movement of valence

electrons in the device.¹ When an electric field is applied across the crystal, a neighboring valence electron can move into the vacancy created by the ionization, and then another can move into the newly created hole and so on. When discussing the effect though, it is convenient to discuss the movement of a hole which has positive mass and positive charge. This "hole conduction" is in addition to the conduction-band electron conduction; therefore, a single ionization event leads to the production of two charge carriers: the hole and the electron. The reverse process is also possible. This is called recombination and occurs, in this case, when a free electron falls into a hole in the valence band. As a result, both carriers are lost.

The amount of current that can be carried by free electrons and holes is proportional to their number, n and p respectively. The number of these intrinsic carriers ($n_i = n = p$) under equilibrium conditions is approximated by:¹⁰

$$n_i = N \exp(-E_G/2kT) \quad (3.1)$$

where

N = Number of Silicon atoms

E_G = gap energy (1.4 eV in Si)

k = Boltzman's constant

T = Temperature in Kelvin

When certain impurities, even in very small amounts, are added to a silicon crystal, they replace silicon atoms in the lattice and the electrical properties of the crystal are drastically affected. If the impurity is from column V in the periodic table, its atoms have one more electron than silicon atoms. When an impurity atom is substituted for a silicon atom, four of its valence electrons are involved in covalent bonds, but the fifth atom is only loosely bound by the

¹ Frequently the bubble analogy is used to explain the use of the hole construct. When analyzing the motion of fluid around a void, it is often easier to consider the motion of a "bubble" than to detail the motion of the surrounding liquid. This holds true for holes; it is easier to investigate the movement of holes than it is the movement of valence electrons.

weak coulomb attraction. That means the fifth electron can be easily elevated into the conduction band.

There is one commonly used method of calculating the ionization energy which must be imparted to the electron to boost it into the conduction band. That is to liken the phosphorus atom to a hydrogen atom immersed in a dielectric medium.¹¹ The result of such calculations are remarkably close to the values obtained experimentally. For example, a typical column V impurity is phosphorus which, when bound in a silicon lattice, has a gap energy of only 0.05 eV for the first electron as opposed to 1.4 eV for silicon. Because of this low ionization energy, the impurity atoms are usually all ionized at room temperature.

By assuming that the donor atoms are all ionized at room temperature, if the number of donor (phosphorus) atoms (N_D) is much larger than n_i , the total number of carriers in a doped crystal will be dominated by those from the phosphorus. In fact, since $N_D \gg n_i$ the number of free electrons can be approximated by N_D . Similar results can be obtained by using certain other column V impurities.

The material obtained when a column V element is combined with silicon is called an n-type material since the free carriers have a negative charge. Another type of semiconductor can be made by using a column III impurity. In this case, there is an electron missing from the bond between the impurity and the four adjacent silicon atoms. This creates a hole. Since the free carriers in this material are positive, it is called p-type material. It should be noted, however, that although both of these materials have mobile charges which are free to move about, the material exhibits what is called space-charge neutrality because any arbitrary volume of the material is electrically neutral.¹⁰

P-N Junctions

When pieces of equally doped p-type and n-type material are placed together, the free negative charges and the free positive charges (in the n- and p-type materials respectively) close to the p-n junction are attracted to

one another. These free carriers diffuse across the junction and recombine (see Figure 5) leaving the "uncovered" ionized impurity atoms locked in the crystal. This destroys the space-charge neutrality of the material near the junction and causes the p-type material to be slightly negative and the n-type material to be slightly positive. (Recall that there are fixed positive charges and free negative charges in n-type material.) This process continues until a region which is depleted of free carriers (the depletion region) is created and the uncovered positive charge in the n-type material generates an electric field which repels the positive free carriers in the p-type material, and vice-versa.¹²

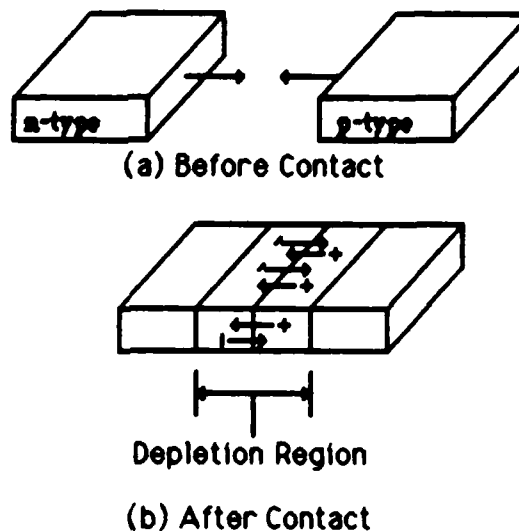


Figure 5: N and P Type Materials Before (a) and After (b) Contact

The electric field created by these uncovered regions generates a "barrier potential" across the junction (see Figure 6). If the junction is reverse biased (a positive potential applied to the n-type end at $x=W/2$ in Figure 6), the magnitude of the barrier potential will increase. On the other hand, if a positive voltage is applied to the p-type material end of the junction (forward biasing the junction), it will have the effect of reducing the height of the potential hill. As the magnitude of the barrier potential approaches zero, current will begin flowing through the junction. The fact that current will only flow in one direction across the pn junction is the basis of semiconductor electronics.

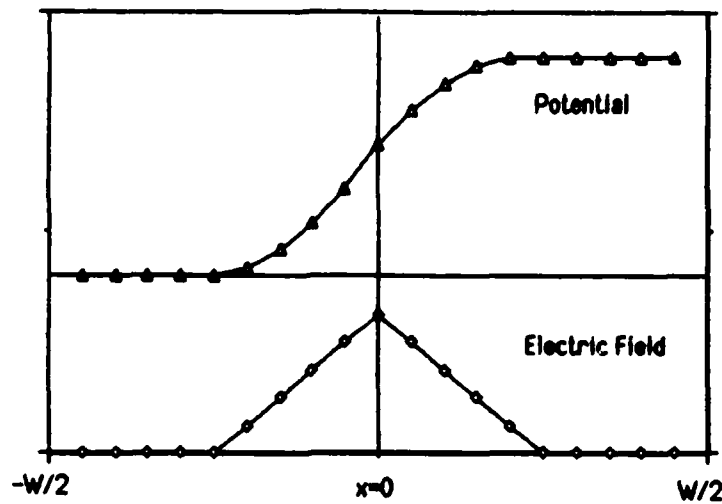


Figure 6: Electric Field and Barrier Potential Across a Depletion Region of Width W

The width of the depletion region is determined by the applied voltage and the density of the impurities in the material. It is a valid approximation to assume all of the applied reverse-bias potential is dropped over the depletion region. This assumes that the bulk material, the part not involved in the depletion region, is a perfect conductor. Although this is not totally true, the resistivity of the depletion region is so much greater than the resistivity of the bulk that virtually no voltage is dropped across the bulk.⁹

As the reverse bias is increased, the width of the depletion region increases until the electric field generated by the uncovered carriers will support the applied bias. That is, if the E -field is as shown in Figure 6 and the width of the depletion region is given by W , then:¹¹

$$V = \int_{-W/2}^{W/2} E \, dx \quad (3.2)$$

where V is the potential applied across the device.

Up to this point we have assumed that the number density of the impurities in each of the material types is the same, but that is not always the case. If both of the number densities are the same, the depletion regions on each side of the p-n junction are the same width. In the case, for example, that the n-type side is doped more heavily, the fixed ion density is greater. Since the number of uncovered fixed charges on each side must be equal to maintain conservation of charge (recall that it is when the free charges from each side recombine that the fixed charges become uncovered), the width of the uncovered region on the n-type side must be narrower.

There are a few other points that will come up later that I will cover here. Up to now, we have assumed that the two pieces of silicon material just exist, then they are doped and put together. In fact, it is essential that the silicon material is of the same crystal form throughout the device. That is accomplished by melting a vat full of silicon and dipping a seed crystal (one having the same crystalline structure throughout) into the melt. The molten silicon attaches to the seed, taking the same crystalline structure as the seed. After the molten silicon has been pulled into a long cylinder, it is cleaned and sliced into wafers.

Some times the manufacturer needs to add more silicon to the wafer. This is done by placing the wafer in an enclosure filled with a silicon vapor. The silicon vapor attaches to the wafer and this new silicon takes the same grain pattern as the wafer. This "grown" silicon is called an epitaxial layer.

After the wafer has been formed, the wafer must be doped with the impurities. There are several ways to do this, but VD MOSFETs are doped by diffusion. Usually, a silicon dioxide layer is grown over the top of the device and then the silicon dioxide is chemically etched away in the areas over where the dopant is wanted. The wafer is then put into an enclosure filled with a gas of a dopant material. If a wafer is placed into a chamber filled with phosphorus gas for example, the phosphorus will diffuse into the wafer making n-type material. The depth of the diffusion is determined by the time the wafer is left in the chamber and the temperature of the wafer/gas system. Usually, the wafer is etched, and doped several times.

CHAPTER 4

FIELD-EFFECT TRANSISTORS: THEORY, CHARACTERISTICS, AND DESIGN

Although the bipolar¹ transistor (the type found in your radio) was developed first, the concept of field-effect devices pre-dates the bipolar concept. As early as 1935, Lillienfeld and Hell each proposed a device which was akin to MOS transistors and, in 1939 Shockley invented his first transistor which was also a field-effect device.¹¹ In fact, much of the early transistor research was based on the field-effect phenomenon.

The first transistor to be produced, though, was a point-contact device presented by Brattain, and Bardeen of Bell Labs on December 16, 1947.¹¹ Due to the fragile and somewhat temperamental nature of the point-contact transistor, it was quickly replaced by the alloyed transistor which was proposed by William Shockley, also of Bell Labs, just one month later -- January 23, 1948.¹¹

Efforts to develop a field-effect device continued to be frustrated throughout the 1950s. This was primarily caused by failure to achieve the low doping levels required to obtain an inversion-layer conducting-channel.¹¹ The first feasible MOSFET was proposed in 1958 by Warner, Atalla, and Schelbner working at Bell. Finally, MOSFET devices became available in the early 1960s.

Characteristics of a MOSFET and the field effect phenomenon will be presented this chapter. The discussion will then lead to an explanation of the design of modern VD MOSFETs. After developing an understanding of the operation of these devices, the manner in which ionizing radiation affects certain MOSFET parameters will be explained. Further information on these subjects can be found in standard MOS texts like Semiconductor Power Devices (ref 9) and Modern MOS Technology (ref 13).

¹ Bipolar refers to the importance of both majority and minority carriers in conventional transistors. Field-effect transistors involve only majority carriers and are called unipolar devices.

Characteristics of MOS Transistors

FETs work much more like vacuum tubes than do the more familiar bipolar transistors. The primary difference in the operation of these two types of transistors is that bipolars are current controlled devices whereas FETs are voltage controlled devices.¹⁶ The following discussion is based on an n-channel FET, but a similar discussion holds for a p-channel device.

Recall that if a piece of n-type and a piece of p-type material are joined together, under normal conditions current can only flow in one direction through the junction. The structure of a FET is based on a double junction like the one shown in Figure 7. It is easy to see that, under normal conditions,

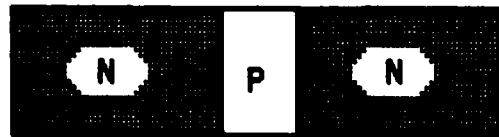


Figure 7: Double (N-P-N) Junction

no current can flow through this device. For example, if a positive voltage is applied to the left end of the device, the p-n junction closest to that end is reverse biased. Since the device is symmetric about the center line, the same argument holds if the voltage is applied to the opposite end.

Now, if an insulator (like SiO_2)¹ is laid down above the p-type region and a conductor (like metal) is placed on top of the insulator, the device would look similar to that shown in Figure 8. If however a negative potential is applied to the conductor (gate), the mobile positive carriers in the p-type material are attracted toward the surface. This is called an accumulation condition.¹³ As one might expect, when the gate bias is changed to a small

¹ The basic operation of a MOSFET relies on an extremely high quality insulator. SiO_2 has extremely high resistivity. It will be shown later that the oxide purity plays a central role in the effect of radiation on MOSFETs.

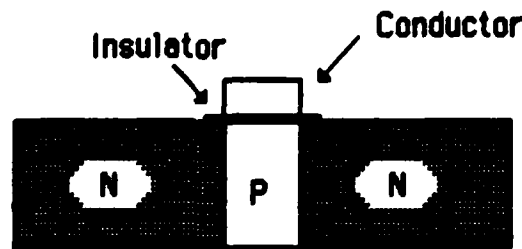


Figure 6: N-P-N Junction with Conductor above the P-Type Material

positive value, the positive carriers are repelled, forming a depletion layer. If the positive potential is increased sufficiently, a layer of negative charge is induced at the surface of the device, just below the insulator.¹¹ This is the result of the field effect and is the same phenomenon which induces the build-up of charge on the opposite sides of the dielectric in a capacitor. This "inversion layer" is now n-type material and is capable of conducting current between the two n-type regions (see Figure 9).

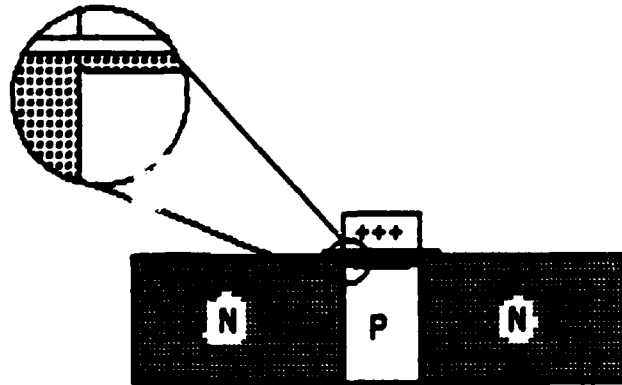


Figure 9: N-P-N Junction with N-Channel

By removing the positive potential from the conductor, the n-channel is eliminated and the flow of current is stopped. Increasing or decreasing the magnitude of the potential will vary the density of the free carriers in the channel. This ability to vary the carrier density in the channel provides a mechanism for controlling the amount of current flowing through a circuit. What I have just described is a simple model of a MOSFET where the ends of

the device correspond to the drain and source terminals, and the conductor above the p-type material corresponds to the gate.

Power MOSFET Design

MOSFETs have been available since the early 1960s and have found many low-power applications, especially in digital circuitry. The roadblock to developing high-power MOSFETs was that materials which could hold off high voltages when the device was in the off state had high values of on-resistance (the resistance between the drain and source when the device is turned on). The primary intended application of power MOSFETs was compact, light-weight power supplies. If the on-resistance of the devices was high, the transformers they would be coupled to in the power supplies would have to be large, eliminating the advantage of using MOSFETs.

Only for the past few years have devices been available which have a low on-resistance and yet are capable of holding off high-voltages. In the early 1980s International Rectifier Company (IRC) developed one of the first power MOSFETs. These vertically-double-diffused devices (called HEXFETs by IRC) were actually hundreds of elementary MOSFETs connected in parallel. Even though these devices are composed of many MOSFETs, the entire device is called a VD MOSFET, or more commonly, a power MOSFET.

Although there have been several improvements in the manufacture of VD MOSFETs since their introduction, the basic construction of MOSFETs today differs very little from the original concept. Figure 10 is a diagram of two of the FET bodies in a VD MOSFET. It shows the doping of the device as well as the metal contacts, the oxide insulators, and the polysilicon gate conductor which is now used in place of the earlier metal gate conductor. These devices are manufactured by first growing an epitaxial n^+ -type region on a n-type wafer. Next, the p-type gate-body regions are diffused rather deeply into the "epi" layer and then the n-type source regions are diffused into the gate bodies. Finally, the oxides and the polysilicon are grown as needed.

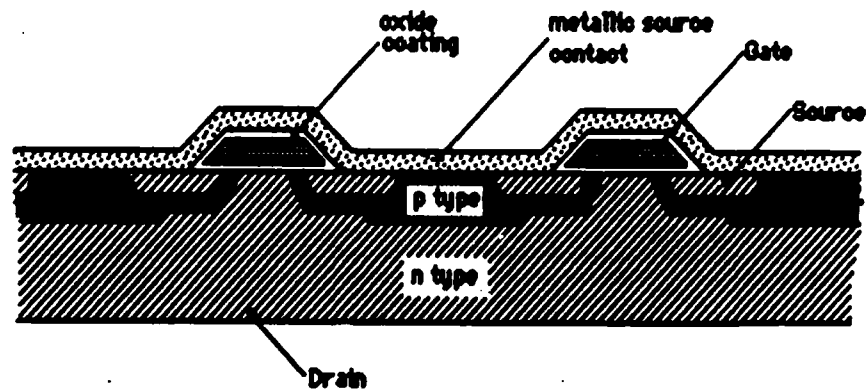


Figure 10: Schematic Diagram of a VD MOSFET

Figure 11 (a) describes pictorially the way one of these FETs operates. Figure 11 (b) shows the current path through one gate body, though it is clear that if there is sufficient potential applied to the gate conductor to allow current to flow through one of the gate bodies, current would undoubtedly flow through the other one.

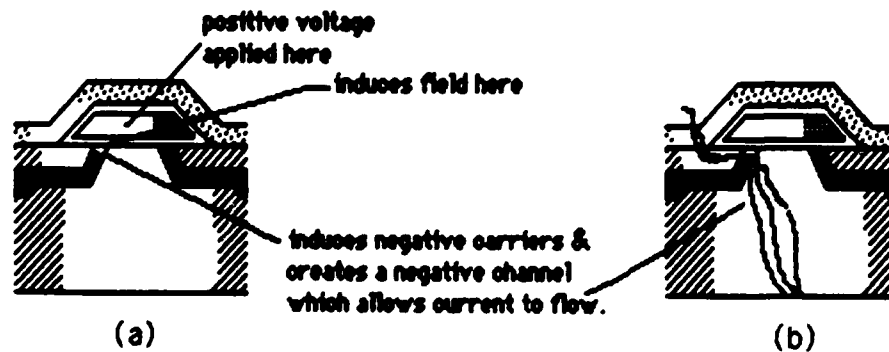


Figure 11: Operation of a Power MOSFET

Radiation Effects

Fortunately, MOSFETs are fairly resistant to neutron induced damage. Moderate fluences (less than about 10^{11} n/cm²) usually introduce insignificant changes in the operating parameters. Above this fluence, the neutron induced

changes in the operating parameters. Above this fluence, the neutron induced dislocations in the silicon lattice increase the on-resistance of the device slightly.¹⁵ These problems are most pronounced in devices that already have higher on-resistances, like high-voltage FETs.

The most significant radiation damage in MOSFETs is caused by gamma radiation. Actually, MOSFETs can be greatly affected by moderate gamma doses. The gamma radiation primarily affects two parameters of the MOSFET: the threshold voltage and the breakdown voltage.

Threshold Voltage

As I mentioned in the discussion about the field-effect, if a "sufficient" positive potential is applied to the gate of an n-channel MOSFET, an inversion layer is induced and conduction can occur. At potential values below that "sufficient" level, the induced negative charges recombine with the positive free carriers in the p-type material, creating an induced depletion region which increases in width with increased gate potential. The magnitude of the "sufficient" potential is called the threshold voltage (V_{TH}). At applied gate voltages below V_{TH} , (effectively) no current flows through the gate-body region. At potentials above V_{TH} the n-channel is induced and current can flow.

During irradiation, gamma photons interact with silicon atoms throughout the device; typically, a photon ionizes the atoms it interacts with. Throughout the majority of the device, the electrons and the holes resulting from the ionization events are either driven by the applied field and swept from the FET, or recombine in the absence of an electric field. Under most circumstances the increase in current caused by the additional carriers resulting from these gamma events is insignificant, so the events have a negligible effect on the FET.¹

¹This assumes that the gamma flux is moderate. If the MOSFET is subjected to a very large gamma pulse (for example 10^{10} rads(Si) per second) there are so many electron-hole pairs generated that a very large current pulse occurs. This could damage the device to the extent that it is unusable.

Ionizations also occur in the gate oxide and the result of those interactions is not negligible. If there is no electric field present, recombination can occur and the electron and hole vanish. Otherwise, the electrons usually are swept from the SiO_2 without much difficulty. The holes, on the other hand, are less mobile in the oxide and are impeded by the silicon/silicon-dioxide interface. A phenomenon known as "oxide-trapped charge" develops where the positive charges build up at the interface. This creates a positive potential at the interface which adds to the voltage applied to the gate and tends to decrease the threshold voltage of n-channel devices and increase the threshold voltage of p-channel devices. This trapped charge also affects breakdown voltage on field plate structures, and was the basis of the model used by Benedetto. The magnitude of this effect is proportional to the density of the trapped charge.

Several parameters can affect the magnitude of the oxide-trapped-charge induced change in V_{TH} . For example, The trapped holes may eventually diffuse through the interface, so that the oxide-trapped charge density eventually equilibrates. Also, increasing the magnitude of the electric field increases the rate of transport of the free charges. This decreases the probability of recombination and increases the rate of trapped charge build-up at the interface. Both of these changes increase the equilibrium density of the trapped charge. If the source of radiation is removed, the trapped charge continues to recombine and diffuse through the interface, thereby decreasing the trapped charge density. This is called annealing and is accelerated by increasing the temperature of the device.

At the same time, a competing, though less well understood, phenomenon may occur. The gamma radiation causes the creation of amphoteric traps at the Si/SiO_2 interface, which are called interface states. In n-channel MOSFETs these interface states introduce a negative potential causing the threshold voltage to change in the opposite direction of the oxide trapped charge. Since these two phenomena (oxide trapped charge and interface states) are of opposite sign and have different rates of generation, the effect of radiation on threshold voltage can be rather complex.

In most cases, the threshold voltage of n-channel FETs decreases with increasing dose until, at some point the threshold voltage drops to zero and the device becomes a depletion-mode device. An depletion-mode device is one which is nominally turned on and a negative potential must be applied to the gate to turn it off. P-channel devices, on the other hand, usually experience an increase in threshold voltage since both the oxide-trapped charge and the interface states increase the positive surface charge. Ionizing radiation makes p-channel devices harder to turn on and cannot cause them to enter the depletion mode.

Avalanche Breakdown

In the explanation given earlier, it was shown that once a FET had been constructed, no current would flow through the p-n junctions unless there was a positive potential applied to the gate. That neglects the fact that there is a continual process of thermally-induced electron-hole pair generation and recombination going on throughout the silicon. If one of these thermally-induced free electron-hole pairs is created in the depletion region, the pair will move apart under the effect of the applied field. This flow of carriers is called leakage current and usually is insignificant.

The thermally generated carriers, like all carriers flowing through the semiconductor, bounce around in the silicon lattice. They are accelerated by the applied potential, travel some distance and then collide with one of the lattice atoms or an impurity, give up some of their kinetic energy to the lattice and then accelerate again until they collide with another atom. If the potential applied across the junction is sufficiently high, however, the carriers are accelerated until they are energetic enough to break loose one of the strongly bound electrons from the silicon lattice in the junction. If the potential is high enough to accelerate the carriers to these energies between each collision, the carriers that are broken loose will also gain that much energy and will break loose another carrier in their next collision. With a sufficiently large potential applied, this process continues until the FET no longer has any control over the current.

This is called avalanche breakdown, because there is no way to stop the

flow of current through the device without decreasing the drain-source potential. Avalanche occurs when the electric field exceeds some critical value (E_c) which is about 3×10^5 V/cm for silicon. Since understanding the effect of radiation on breakdown voltage is the aim of this research, it is important to present a model of this phenomenon.

As an illustration, consider a single electron-hole pair which is thermally generated at some point x in the depletion region (see Figure 12). If a potential has been established across the device, the electron will be driven toward the n-type material and the hole

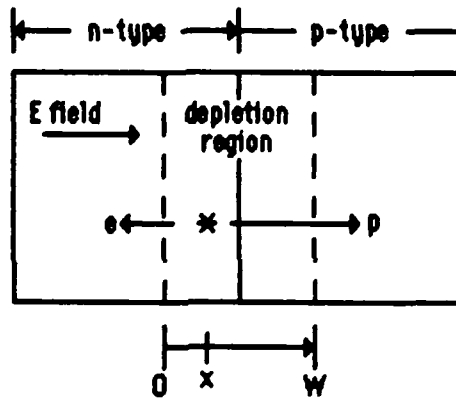


Figure 12: Thermally Induced Ionization Effects

will be swept toward the p-type material by the electric field. If these carriers are sufficiently accelerated, the number of subsequent ionizations they generate can be characterized by the expressions:⁹

$$\alpha_n = 80 e^{-b/E} \quad (4.1)$$

and

$$\alpha_p = 80 e^{-b/E} \quad (4.2)$$

where α_p and α_n are the number of electron hole pairs created per centimeter traveled in the direction of the E field by holes and electrons respectively, and E is the magnitude of the electric field. In silicon, with E between 5×10^4 and

8×10^5 V/cm, the values of a , b , and δ are:⁹

$$a = 1.6 \times 10^6 \text{ cm}^{-1}$$

$$b = 1.65 \times 10^6 \text{ V cm}^{-1}$$

and

$$\delta = 0.344.$$

Since each electron-hole pair which is generated will also experience the same acceleration as the original pair, the average number of electron hole pairs ($M(x)$) resulting from one thermal ionization at location x is given by:⁹

$$M(x) = \int_0^x \alpha_n M(x') dx' + \int_x^W \alpha_p M(x') dx' + 1 \quad (4.3)$$

Then, differentiating both sides we obtain:

$$\frac{dM(x)}{dx} = (\alpha_p - \alpha_n) M(x) \quad (4.4)$$

Solving this equation and letting $M_0 = M(x=0)$ we can obtain another expression for $M(x)$:

$$M(x) = M_0 \exp \left[\int_0^x (\alpha_p - \alpha_n) dx' \right] \quad (4.5)$$

Substituting (4.5) into (4.3) for $M(x')$ and solving (3) for at $x=0$ we find

$$\frac{1}{M_0} = 1 - \int_0^W \alpha_p \exp \left[\int_0^x (\alpha_p - \alpha_n) dx' \right] dx \quad (4.6)$$

Now, substituting (4.6) for M_0 in (4.4) we arrive at a closed form solution for $M(x)$:

$$M(x) = \frac{\exp\left[\int_0^x (\alpha_p - \alpha_n) dx'\right]}{1 - \int_0^W \alpha_p \exp\left[\int_0^x (\alpha_p - \alpha_n) dx'\right] dx} \quad (4.7)$$

This is an expression which yields the multiplication resulting for a single ionization event. Multiplication in a semiconductor is the basis for semiconductor radiation detector systems; however, in a detector one strives to achieve a known, finite multiplication value. Avalanche breakdown, on the other hand, is defined to occur when the multiplication approaches infinity:

$$M(x) \rightarrow \infty \quad (4.8)$$

In our model, to yield an infinite value of $M(x)$ the denominator of (4.7) must go to zero, or

$$\int_0^{W'} \alpha_p \exp\left[\int_0^x (\alpha_p - \alpha_n) dx'\right] dx = 1 \quad (4.9)$$

Since the width of the depletion region changes with the applied voltage, W' indicates the width of the depletion region when the applied potential is equal to the breakdown voltage.

This avalanche effect will cause a very large number of carriers to be formed and will allow current to flow through the FET until the potential is removed. If no permanent damage was done to the device during this breakdown condition, the device will operate properly once the current flow has been stopped. Frequently though, large currents flow through the junction during breakdown. When this happens the resistance of the device materials causes too much power to be dissipated in the junction and the device is destroyed.

In a MOSFET, the avalanche breakdown usually occurs at the edge of the

device where the p-n junction and the depletion region are sharply curved.¹⁴ In that region the potential is dropped over a smaller spatial region which causes the electric field to be larger. Since the field is larger, the onset of breakdown is earlier because E_c is exceeded in the curved region first. There are two ways to increase the breakdown voltage of a power MOSFET: increase the thickness of the device or incorporate an electric field termination technique at the edge of the device which approaches an ideal electric field termination.¹⁶

Increasing the device thickness increases the on-resistance.¹⁶ It was explained earlier why increasing the on-resistance is not a suitable solution for developing a high-voltage MOSFET. Therefore, in order to increase the breakdown voltage several techniques are used to terminate the field lines in a manner which will increase the breakdown voltage. In the next chapter the types of field terminations most commonly used in power devices (including bipolar transistors, diodes, and thyristors as well as MOSFETs) will be presented. The effect of radiation on each of these techniques will also be considered.

CHAPTER 5

FIELD TERMINATION TECHNIQUES

The purpose of a field termination technique is to improve the breakdown voltage of a p-n junction. In this chapter I explain the reason terminations are needed and describe the types of terminations used most frequently in power devices. I have excluded etched junctions, a method where some of the silicon is removed from the device, from the discussion because the tolerances are so critical that the procedure is not generally used in commercial devices. I have included field ring, field plate, and junction termination extensions in the discussion.

The goal of the semiconductor engineers who employ termination techniques is to achieve the breakdown voltage of a plane junction. In a device with a plane junction, the junction has no curvature (see Figure 13) so the electric field lines are all parallel and no region develops a critical field strength (E_C) before the entire region develops E_C .

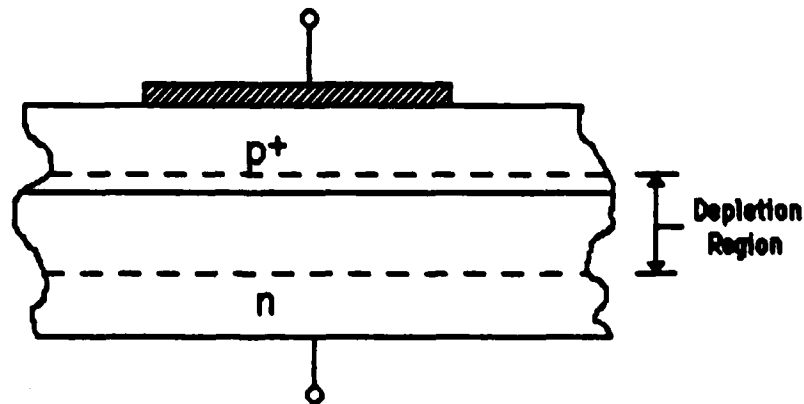


Figure 13: Example of a Plane P-N Junction

In a non-plane junction, the junction, the depletion region, and the electric field are curved (see Figure 14). This curvature creates localized regions where the field gradient is steeper, thereby causing those regions to develop E_C long before the remainder of the junction approaches E_C . The magnitude of this effect depends on the ratio of the depletion width to the curvature so that

It is much more severe for high voltage devices (depletion width varies as the square root of the applied voltage). By properly employing field terminations, the designer can modify the shape of the electric field in the region where the curvature is most severe, thereby increasing the breakdown voltage.

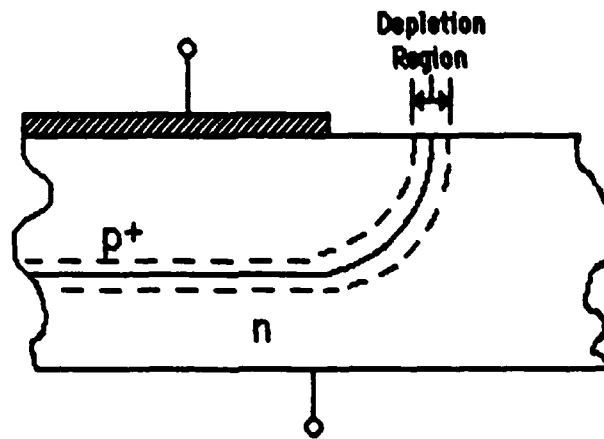


Figure 14: Example of a Curved P-N Junction

The shape of the electric field can be modified by incorporating additional structures in or on the FET chip. The most commonly used techniques are Field Rings (FRs), Field Plates (FPs), and Junction Termination Extensions (JTEs). The maximum effect these techniques can achieve is to attain the same breakdown voltage as a similar device without a curved (or with a plane) junction. Additionally, the amount of increase in V_{BD} that can be obtained by using termination techniques depends on the voltage rating of the FET. In lower voltage devices, the terminations do not improve V_{BD} much; however, the improvement obtained in a high-voltage device using terminations can result in a V_{BD} as much as twice the V_{BD} of the same device without terminations. Since the maximum effect of radiation is to negate the effect of the termination, the effect of radiation can be expected to be more significant in high-voltage devices.

Field Rings

Field rings are a sequence of ring shaped doped regions which circle the edge of the chip (see Figure 15). In some applications there may be several rings, while in other cases one ring may be sufficient.¹¹ The dopant used in the field rings is the same as that used in the bulk gate region.

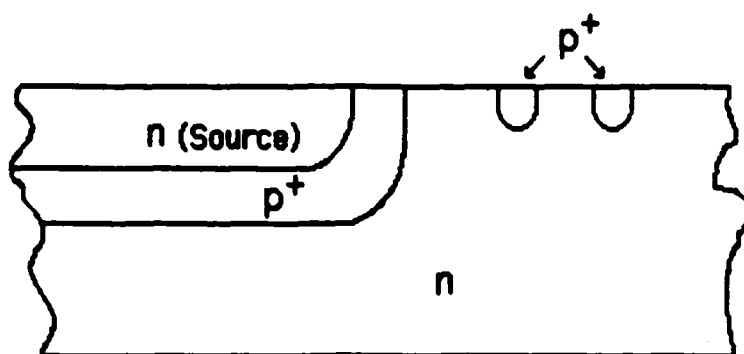
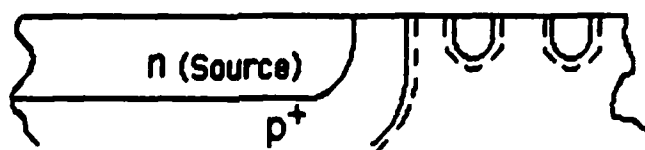
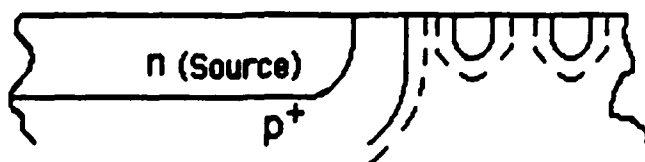


Figure 15: Example of a Field Ring Termination

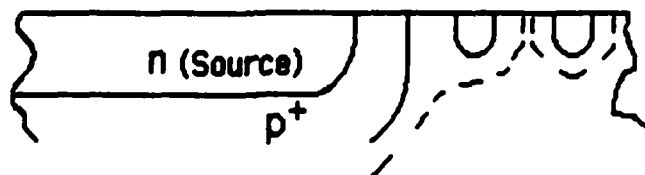
The field rings are allowed to electrically float just like the bulk gate regions. As the potential across the chip increases, the depletion region of the p-n junctions around the bulk gate and around the field ring(s) widen (see Figure 16 (a) and (b)).



(a)



(b)



(c)

Figure 16: The Depletion Region Shape with (a) No V_{DS} , (b) Moderate V_{DS} , and (c) After Punch-through

At some point, just before the same FET without field rings would breakdown, the depletion regions for the bulk gate region and the field ring meet and "punch-through" occurs.¹⁷ As even more potential is applied across the FET, the depletion regions widen further until the region punches-through to the second field ring and so on.

A single, optimally positioned field ring can significantly improve the performance of a device as you can see in Figure 17.^{9,17} If the ring is not optimally positioned though, the improvement in breakdown voltage due to the field ring can be negligible (see Figure 18). Additionally, if there

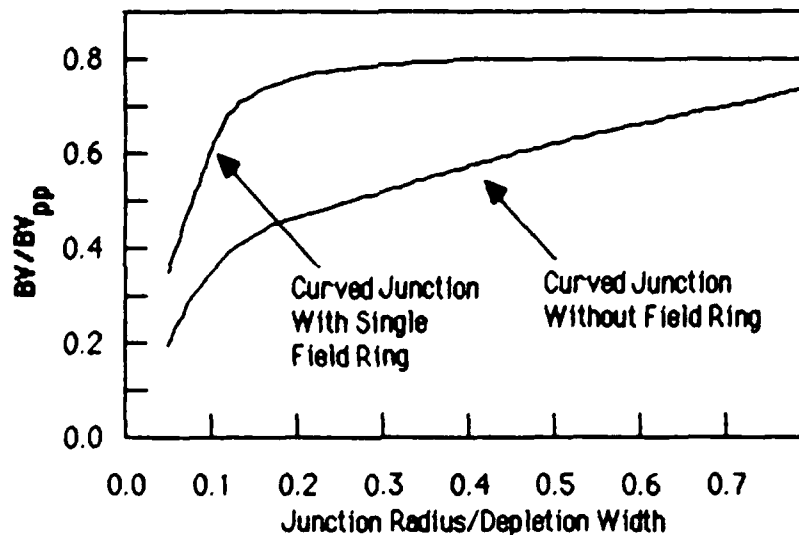


Figure 17: Breakdown Voltage of a Curved Junction With and Without Field Rings [Adapted from Semiconductor Power Devices (ref. 9)]

are any surface charges (for example oxide trapped charge above the field rings) the electrical fields generated by the charges can perturb the field ring configuration and thereby change the breakdown voltage of the device.

As a FET with field ring terminations is irradiated, interface states develop which effectively introduce negative charges into the structure. If the rings are in the optimum position, the perturbation that occurs because of these charges can decrease the breakdown voltage of the devices. Alternatively, if

the rings are not in the optimum position the negative charges can either improve or degrade the effectiveness of the field rings.

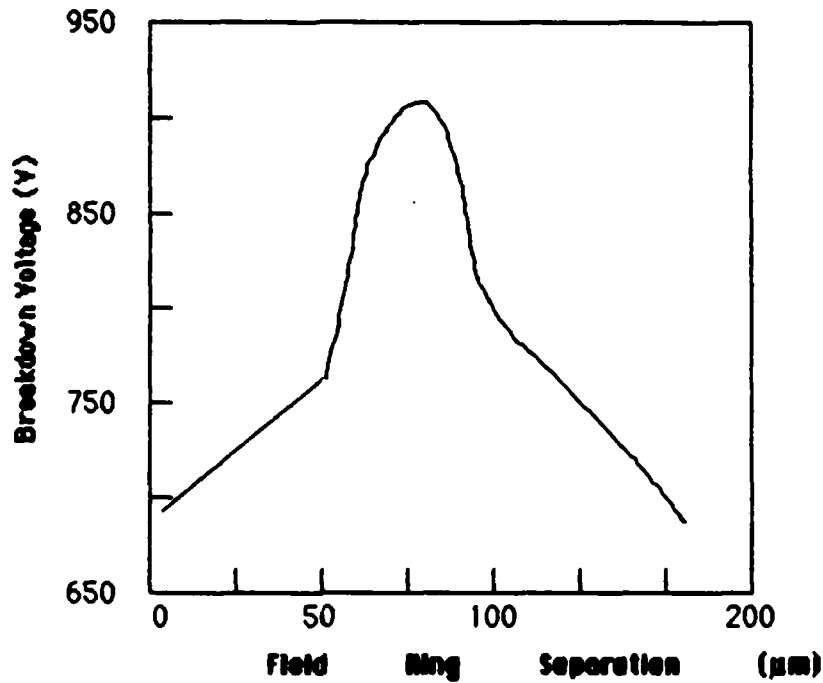


Figure 18: Sensitivity of Field Ring Placement
[Adapted from Semiconductor Power Devices (ref. 9)]

Field Plates

The operation of a field plate is somewhat analogous to the operation of a MOSFET gate. For the purpose of demonstration, imagine an n-channel power MOSFET with a conductor placed above and insulated from the undoped region at the edge of the chip (see Figure 19). Recall from Chapter 3 that for any given voltage, the width of the depletion region is determined by the free carrier density ($N_D \text{ cm}^{-3}$). When a negative voltage is applied to the field plate, some of the free carriers are repelled, decreasing the free carrier density, thereby increasing the width of the depletion region.

Since the potential is usually low, the widening of the depletion region occurs near the surface of the chip. This increases the breakdown voltage by decreasing the curvature of the depletion region. An effective field plate

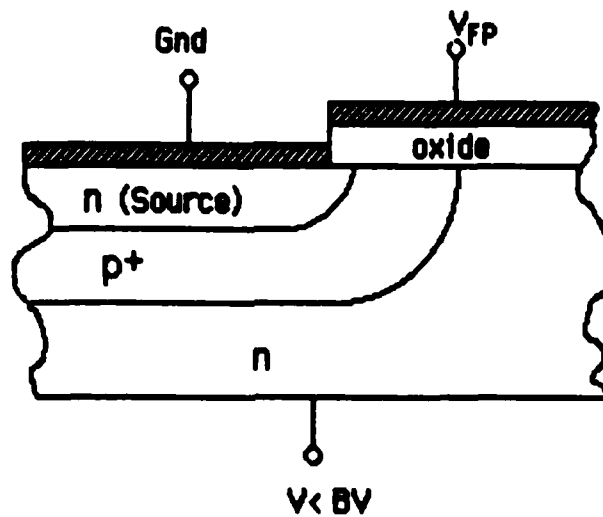


Figure 19: Example of Field Plate Termination of a P-N Junction

will cause the depletion region to be nearly horizontal near the surface of the device and cause the breakdown voltage to approach that of a plane junction.⁹

The similarity between field plates and FET gates continues into the effect of radiation. There are similarities between the effect of radiation on the threshold voltage of a FET and the breakdown voltage of a FET with field plate terminations. The effect of trapped charge causes the breakdown voltage in n-channel FETs to decrease. If substantial numbers of interface states are also produced, the breakdown voltage may subsequently recover to some extent. In his paper, Blackburn states that the electric field in the field (plate) oxide traps the holes that are created there by gamma photon ionization of silicon atoms.⁸ This is equivalent to applying an increasingly positive potential to the plate.

In an n-channel device, the positive trapped charge increases the number of negative free carriers in the bulk material thereby narrowing the width of the depletion region and decreasing the breakdown voltage. As the irradiation continues, negative interface states are created, increasing the negative potential as well as the breakdown voltage.⁸ In a p-channel device, both the oxide trapped charge and the interface states are positive. Since the application of a positive potential to the field plate of a p-channel device

decreases the number of free carriers in the bulk, the depletion region widens and the breakdown voltage increases.

The number of oxide trapped charges can be calculated using the method proposed by McGarrity.⁵ That is, the number of trapped holes (N) is given by:

$$N = D t_{ox} A G F \quad (5-1)$$

where

D \equiv dose (rad(SiO₂))

t_{ox} \equiv oxide thickness

A \equiv Field plate area

G \equiv electron hole generation constant

F \equiv fractional number of holes trapped in the oxide

Then it can be shown that the change in breakdown voltage caused by the trapped charge is:¹⁸

$$\frac{\Delta V_B}{V_B} = \frac{\sigma}{\epsilon E_c} = \frac{q D t_{ox} G F}{\epsilon E_c} \quad (5-2)$$

Junction Termination Extension

The junction termination extension technique also improves the breakdown voltage of a MOSFET by decreasing the number of free carriers in the bulk material. In a JTE, though, the free carrier density is modified by implanting ions of the opposite sign into the bulk material so that they recombine with the free carriers (see Figure 20). A sufficient number of ions is implanted so that the free carrier density is changed to between 0.6 to 0.8 $\epsilon E_c/q$.⁵ This reduces the number of available charges in the lightly-doped region to a number below the amount required to balance the uncovered charges in the n-type region. As in field plates, this decreased free carrier density increases the depletion region width and increases the breakdown voltage.

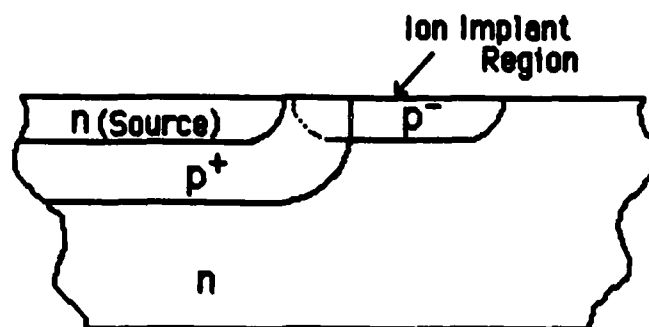


Figure 20: Example of a Junction Termination Extension

The effect of gamma radiation is to increase the free carrier density. When the number of carriers is increased to the original value, the device operates as if there was no JTE. Again, by using McGarrity's technique we can write an expression for the dose required to return the device to its unmodified level of free carriers.¹⁶ That is, letting s be the density of radiation induced charges, then from equation (5-2) it is easy to see that:

$$s = q D t_{ox} G F \quad (5-3)$$

When s is, for example $0.2 eE_c/q$ ($1 - 0.8 eE_c/q$) the device would be at its original charge density. This would occur when

$$s = 0.2 eE_c/q = D t_{ox} G F \quad (5-4)$$

or, when the dose is equal to

$$D = 0.2 eE_c / (q t_{ox} G F) \quad (5-5)$$

Since ionizing radiation creates charges of both signs, it has the same effect on FETs of both types. This theory predicts that substantial decreases will occur in the V_{BD} of the device.

CHAPTER 6

EXPERIMENTAL PROCEDURE

Having determined how MOSFETs work, the next goal was to devise an experiment which would expose the MOSFETs to ionizing radiation and then measure the breakdown voltage.

I was fortunate to be working on this project with Allan Johnston of the Boeing Radiation Effects Laboratory (BREL) and Ken Galloway of the National Bureau of Standards. I was also fortunate to be offered the opportunity to perform my experiments at BREL. The engineers (Itzu Aurimura, Wes Will, Mark Baze and Rick Kennerud) and technicians at BREL provided essential help in obtaining the necessary equipment and preparing the experiment.

In order to evaluate the effect of radiation on MOSFETs, I needed to develop a way to measure the breakdown voltage of MOSFETs after they had been exposed to gamma radiation. Before explaining the procedure decided upon, a brief explanation of the procedure used in many earlier experiments and the concerns that motivated us to develop a new procedure will be presented.

Typical Experimental Procedure

Most of the earlier experiments were performed by different organizations and, therefore, different equipment was used. There were, however, many parts of the various test procedures which were similar. In this discussion I will present the general procedure followed by Benedetto,⁷ although as I just implied, it is similar to many of the others.

Typically, one or more FETs were connected to a test fixture which secured the devices and in many cases applied an electrical bias to them. The test fixture would then be placed in a radiation field so that the devices would be irradiated at a known dose rate. After a pre-determined period of time had elapsed, the test fixture was removed from the radiation field. Then the devices were removed from the test fixture and the applied bias. After some

period of time (ranging from seconds to hours), the devices were tested to determine the effect of the cumulative dose on the parameter (eg., breakdown voltage) being evaluated. Some time after the testing had been performed, the devices were returned to the test fixture and the process was repeated several more times.

Before beginning our experiment, Allan and I discussed this "typical" procedure and decided to attempt to improve on it. We decided that there were two aspects that needed to be changed. It has been shown that the damage caused by radiation will go away (anneal) if the devices are allowed to rest, especially at elevated temperatures. Therefore, one concern was that when the electrical bias was removed and the device was allowed to rest between irradiation and measurement the magnitude of the measured effects may be ameliorated by annealing.

Our other concern was based on the number of times the devices were being tested. In the "typical" procedure, the devices are tested at predetermined cumulative doses (eg., Benedetto used 1, 2, 5, 10, 20, 50, ... krad). This scheme would yield only a few measurements (10 in the Benedetto scheme) in 1 Mrad of cumulative dose. Our concern was that important data may be missed between the measurements. These concerns encouraged us to come up with a new experimental procedure. We decided to measure the effects on the devices while they were in the radiation field. In this way the devices were kept biased throughout the experiment, eliminate any annealing, and allow us to test the devices more often without drastically extending the duration of the experiment.

Experimental Procedure and Equipment

Breakdown voltage is determined by measuring the drain-source voltage required to sustain an arbitrary current (1 mA in our case) in a transistor which is turned off. The procedure was based on a 1 mA source connected in series with the parallel combination of a switched load, a digital voltmeter (DVM) and the FET being tested (see Figure 21). The FET being tested was placed in the radiation source and connected to the rest of the circuit by a six foot cable. The load was switched in and out of the circuit by a pulse

generator. The pulse generator was controlled by an IBM PC which also recorded the voltages measured by the DVM. The software I prepared for this experiment was written in Pascal and is presented in Appendix A.

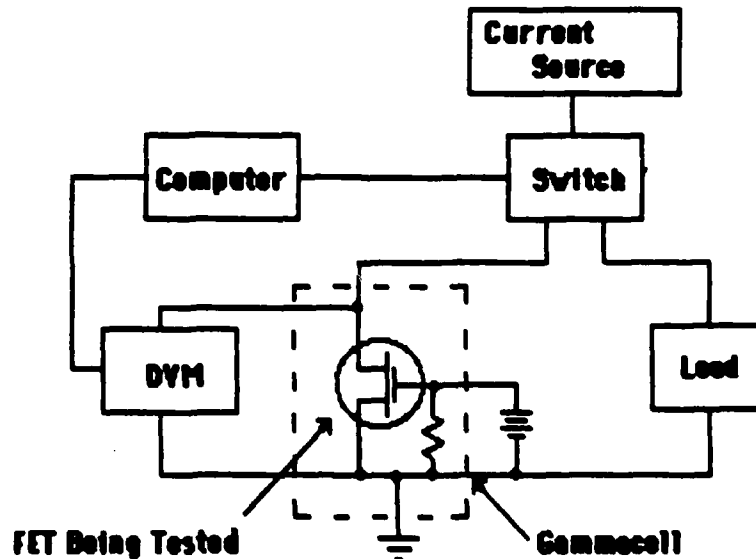


Figure 21: Equipment Setup

The radiation source used was a Gammacell 220 belonging to BREL. It consists of a large number of Cobalt-60 "pencils" which are arranged in a circle in the midplane of a large drum. There are no pencils at the center of the drum so that an elevator holding the sample to be irradiated can be lowered into the gamma flux. The cobalt pencils provide a gamma flux of approximately 200 rads(Si) per second at the center of the drum. The entire Gammacell is shielded by lead so that there is no radiation hazard to personnel using it.

During a particular test, the FET was connected to the mount which was already in the Gammacell elevator. The interconnecting cable was then routed to the controller board and the test equipment was energized. Next the program which controls the experiment was started and then the name of the file the data was to be written to, the dose the FET would receive during the time it was being lowered into and removed from the Gammacell, the dose rate the FET would receive while it was in the cell, and the total dose the FET was to receive (the target dose, usually 100 or 500 krad) were input. Then the

program set the parameters for the pulse generator and DVM (for example, pulse amplitude or voltage range).

Once the equipment had been set up and the controlling program initialized, the FET mount was lowered into the cell. As the elevator reached the bottom of its travel, the computer timing sequence was started. Immediately the computer switched the load out of the circuit so that the entire milliamp of current was routed through the FET being tested. Since this FET was turned off, the drain-source voltage of the FET was its breakdown voltage. The computer then instructed the DVM to measure the drain-source voltage, paused momentarily, switched the load back into the system which biased the FET to 80% of the manufacturers listed V_{BD} , and stored the value the DVM measured. Finally, the clock time, elapsed time, the dose received since the last measurement, the cumulative dose, and the DVM reading were recorded in the data file. The computer then waited until the start of the next measurement cycle. These cycles continued until the cumulative dose exceeded the target dose. When the experiment was over, the computer closed the data file and ended the program. A data file which is representative of the results obtained from an experiment is included in Appendix B.

The Controller Board

The heart of the test equipment configuration was the controller board which we designed and built. It consists of the current source, the switch, and the ports for connecting a high-voltage power supply, the pulse generator, the DVM, and the FET test mount. A schematic diagram of the controller board is shown in Figure 22.

The current supply ($Q1$, $R1$, $R2$, and $CR1$ through $CR4$) was based on negative current feedback through resistor $R2$; the circuit is designed so that the voltage drop across $R2$ is much greater than the threshold voltage of $Q1$. As current flows through $R2$, a voltage is dropped by $R2$ ($V=IR$). V_{GS} is approximately equal to the sum of the voltages dropped by the zener diodes $CR1$ through $CR4$ (approximately 16V) minus the voltage dropped by $R2$ (let $I_D \cdot R_2 = V_2$). If I_D is such that V_{GS} is greater than the threshold voltage of $Q1$ ($16 - V_2 > V_{TH}$), $Q1$ will remain turned on and current will flow.

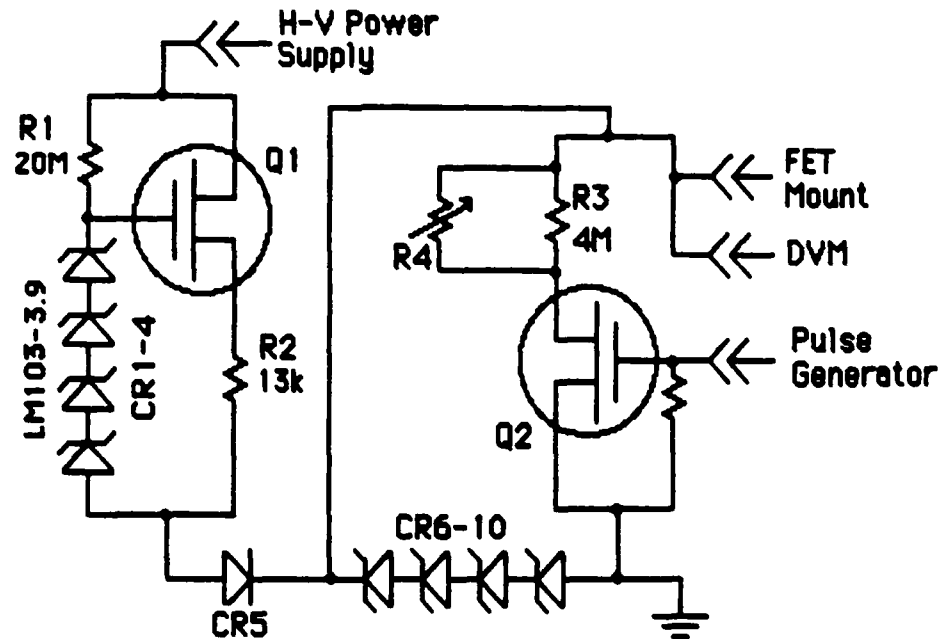


Figure 22: Schematic Diagram of Controller Circuit

As V_2 approaches $16 - V_{TH}$ then Q1 conducts less and the system stabilizes when the on-resistance of Q1 plus R2 times I_D equals 16V. This establishes a constant value for I_D regardless of what the applied high voltage is, so long as it is larger than about 20V.

There are two sets of devices which were included for circuit protection. CR5 acts as a blocking diode in case the high-voltage power supply gets connected with the polarity reversed. CR6 through CR10 provide an alternate current path in case the remainder of the circuit develops an open circuit condition. Since the circuit provides a constant current, if the path for current opens the system will attempt to maintain the current by increasing the voltage to the circuit. This could damage the controller; therefore the high voltage zener bridge was installed for circuit protection.

The remainder of the circuit is the switched load which periodically switches the resistor network consisting of R3 and R4 out of the circuit. The pulse generator is connected to the gate of Q2, the switching FET. In the nominal state, a +5.0V signal is applied to the gate by the pulse generator.

This turns on Q2 and allows current to flow through the R3 and R4 network. The adjustable resistor (R4) provides a means of adjusting the voltage applied to the FET being tested when the load is in the circuit. At the start of the measurement interval the computer would instruct the pulse generator to set the output to -3.5V. This would turn off Q2 and cause the entire 1mA (less the few microamps that would go through the DVM) to go through the FET in the gamma cell. At that point the computer instructed the DVM to measure the voltage between the DVM port and ground which was, by definition, the breakdown voltage of the FET being tested.

The Computer

This test procedure would have extremely tedious and error-prone without a computer controlled test set. The computer coordinated the functions of timing, switching, measuring, and recording in the tireless manner that only computers can achieve.

The original plan was to use a Digital Equipment Corporation MINC computer to control the experiment. The MINC is designed to be used as a test equipment controller and contains many additional features to accommodate circuit analysis and so forth. After preparing a Basic program on the MINC to run the experiment and getting a prototype test set-up running, I found that there was an IBM PC that was available for the experiment. I decided to use the PC because there were several others at BREL and at the University which could be used for program development work, whereas there was only one MINC available. Additionally, there were several data analysis programs as well as a means of transferring the data to other computer systems available for the IBM. These facilities were not available for the MINC.

The IBM was configured with a Ziatech 1448 card which interfaced the computer with IEEE 488 compatible test equipment. The IEEE 488 standard defines the function of the lines on a parallel buss. It also defines a standard connector and an addressing protocol. The standard, in many ways analogous to a programming language like FORTRAN or Pascal, defines certain criteria for manufacturers to follow while allowing the manufacturers to include their own unique enhancements. The result is that complete test equipment

systems can be configured from devices made by different manufacturers and with compatible control commands and data transfer capabilities.

As I mentioned above, the program which controlled the entire experiment was written in Pascal. There were three reasons for this. First, the Pascal language, as implemented on the IBM PC by Digital Research, allows the transfer of data in Byte data types. This is necessary to interface with the Ziatech 1488 card. Secondly, Rick Kennerud at BREL had already prepared several external Pascal procedures and functions which simplified the use of the Ziatech card. Finally, the Digital Research Pascal compiler was available on several of the IBM PCs at BREL. The program source code and a flow chart explaining the purpose of the various sections of it are included in Appendix A.

Auxiliary Tests

There were several auxiliary tests performed during the course of the experiment to test the equipment setup, validate the procedure, verify the results, and to baseline the FETs both before and after they were tested.

Testing the Equipment Setup

After the controller had been designed and assembled, I had to ensure that the circuit performed as it was intended to. The test consisted of connecting the equipment, without the computer, and operating it manually. First I turned the high voltage on to about 50V and measured the current out of the source. It was 0.99 mA, a very satisfactory value. Next I tested the switching function. By manually switching the signal applied to the gate of Q2, I ensured that the load was switched in and out of the circuit when expected. After determining that the circuit was working properly, I went on to verify the entire procedure.

Procedure Verification

Verification of the procedure was a three step process. First, I needed to ensure that there were no thermally induced breakdown voltage changes in conjunction with the changes induced by radiation. Second, I needed to verify that the entire system, the controller, the program, the computer and all the

other test equipment, worked properly throughout an entire experiment. Finally, I needed to prove that the results of our experiment agreed with other measurement techniques such as a standard curve tracer. A curve tracer is a device which looks like an oscilloscope but which displays the voltage versus current characteristics of a device (not necessarily a FET). Although the machine is capable of performing several different tests on all sorts of transistors, I usually biased the gate of a FET so that the device was turned off and then increased the V_{DS} until breakdown occurred, thereby measuring breakdown voltage. Alternatively, I would increase the gate voltage until the device turned on so as to measure the threshold voltage.

When the device is in breakdown, all the power in the system (for example .25 watts if the breakdown voltage is 250V) is deposited in the FET. As with many semiconductors, as the temperature of the FET increases, its resistance increases which causes the breakdown voltage to increase. This would combine with the radiation induced breakdown voltage changes. In order to ensure valid results, I had to show that the interval between measurements was sufficient to allow the device to dissipate any heat built up during a breakdown voltage measurement. I also needed to ensure that the measurement was fast enough that heating devices during the measurements did not cause inaccuracy.

To perform the test I set the FET mount on a table and ran a normal experiment. Having no outside phenomena affecting the breakdown voltage, any change that occurred must be from internal causes. During the test I varied the time between measurements to find out how frequently I could test the FET without having any heating effects. I found that, with a 350V device, as long as there was about seven seconds between measurements there was no adverse effect on the results. It was difficult to determine just how close together the measurements could be made since seven seconds was the minimum time for one computer cycle. The reason there was no heating problem even with only seven seconds between measurements is because the FET was only in a breakdown condition for about 0.2 seconds. Even though this experiment showed that we could make measurements about every seven seconds, we rarely made measurements more often than every 25 seconds

simply because there would be too much data generated otherwise.

In order to ensure that the system worked as we had planned, I performed an experiment, monitored the entire procedure, and checked the results. I chose one of the n-channel FETs to work with and attached it to the test set and lowered the device into the gamma cell. Throughout the experiment I observed the data and timed the measurement cycle to ensure everything was working as intended. At the end of the experiment I verified that the final breakdown voltage measurement agreed with the value measured on a curve tracer. I looked at the data file generated by the experiment and concluded that it appeared valid.

Subsequently, I plotted the results of the first two tests and found that the results contained what could be called low grade noise (see Figure 23). I then performed a few short experiments and found that the delay between the start of the DVM measurement and the time when the computer recorded the value was too short. The problem was that DVM had not always stabilized when the computer recorded the results. To eliminate this problem, I increased the delay which decreased the scatter in the measurements to less than 0.1 volt, the resolution of the DVM.

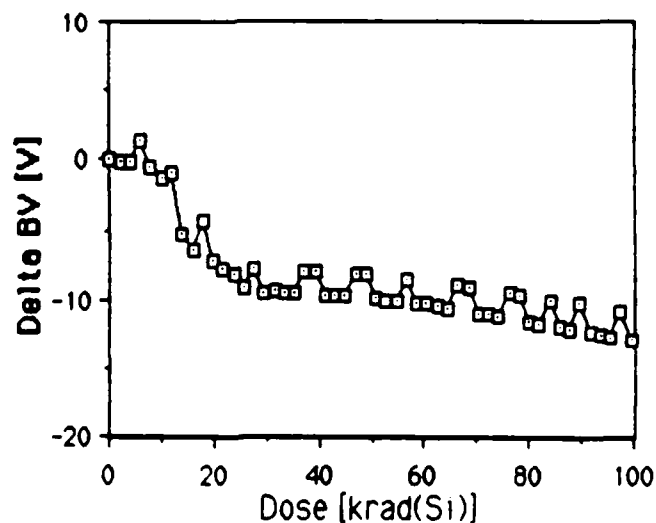


Figure 23: Results of First Experiment Showing Noise

Now that the experimental procedure had been checked out, all that remained was to verify that the results the experiment reported were correct. To do this, I tested most of the FETs on the curve tracer prior to testing them. Later, when I put the FETs in the test set, I checked the breakdown voltage before I put them into the gamma cell. Since there was always good agreement, I knew the test set was correctly evaluating breakdown voltages. I also needed to show that the values reported at the end of the test were correct. To do this I tested the FETs on a curve tracer immediately after the irradiation was complete and compared the results. Recall that one of the concerns was that in the time between removing a FET from the cell and testing it, the change in breakdown could anneal somewhat. If I detected a difference between our final gamma cell value and what we measured on the curve tracer, I would need to determine if annealing had occurred or if some other factor caused the discrepancy.

When the post irradiation tests were performed, I found that the results from the curve tracer agreed extremely well with the last gamma cell reading. In fact, several months later I checked several of the FETs that were irradiated first and found no evidence of significant annealing even then. One must be careful about drawing too many conclusions about annealing from these results though. Since most of these FETs were irradiated up to 500 krad, they were long past the sensitive stage of the change in breakdown when they were removed from the gamma cell. Further testing would be required to determine if FETs which were removed from the cell during a period of rapid change in breakdown would anneal.

Baselining the FETs

Before testing the FETs I baselined many of them. To baseline them, I used the curve tracer to determine both the threshold voltage and the breakdown voltage of each transistor. These values were recorded along with any abnormalities noticed during the baselining procedure.

In some of the experiments, a very large change in the breakdown voltage was noticed. This could be a problem since there was no way to tell during the experiment if the breakdown voltage had actually changed that much, or if the

characteristics of the FET had changed to the point where its leakage current (the current normally that flows even when the device is turned off) was a milliamp. To ensure that the test results were valid, I tested the FETs on the curve tracer after the experiment and found, in every case, that the leakage current was much less than 1 mA.

In some cases the breakdown voltage of the tested FETs fell below the nominal voltage of the system. The breakdown voltage measurements are still valid since, when the switch (Q1) was turned off, the whole milliamp flowed through the FET being tested and the resulting voltage read by the DVM was still the breakdown voltage. The problem was that when the switch was closed so that the device was in its nominal state, the voltage across it was still above the breakdown voltage so that some of the current could have flowed through the FET being tested. This altered the test conditions and may also have caused thermal changes in breakdown voltage. Although the data collected after a device failed in this manner was invalid, the data that was collected before a device's breakdown voltage dropped below the nominally applied voltage was valid; therefore, in the two or three cases where this occurred, there were still pertinent results obtained.

Optical Microscope and Microprobing

Manufacturers in the semiconductor business are not willing to release much information about their devices. According to Chuck Koehler, a sales representative for Supertex Incorporated, there are very few differences between the devices developed by different manufacturers. Therefore, if anything about the design of a FET is known by a competitor, a company's device can be duplicated rather easily. Since we needed to determine the type of termination techniques used in each of the FETs we were testing, and since that is considered proprietary information by the manufacturers, we had to develop a way of determining the type of termination techniques used in each device.

To do this I opened the case of each FET type and inspected the device through an optical microscope. In some cases, when I had determined that

the termination included field plates, it was necessary to determine if the plates were floating (not electrically connected to another part of the FET) or if they were connected to the source or the gate. To do this, I attached microprobes to a mount which was maneuvered using two vernier devices each resembling a micrometer handle. I then connected the microprobes to an ohmmeter. Using the vernier handles to move the probes and a microscope to see the device, I positioned the microprobes so that one was in ohmic contact with the field ring (I verified this by touching the other probe to the field ring at another location) and then connected the other probe to first the source contact and then the gate contact. In this manner I was able to determine if the field plates floated or not.

CHAPTER 7

RESULTS AND DISCUSSION

The original purpose of this research was to verify the effect of the radiation on the breakdown voltage in p-channel VD MOSFETs. It was our intention to use n-channel devices to verify the test procedure and compare our results with those obtained by Benedetto and Blackburn. We also intended to test a new very-high-voltage n-channel device to see if the earlier research was valid in this regime.

As I will discuss later, during the verification phase of the experiment we noticed some variations in the plots of V_{BD} versus dose in the n-channel devices that had not been reported earlier. This, coupled with other characteristics we noticed later, encouraged us to further investigate the effects in n-channel devices using our "improved" test procedure. Therefore, I will first present the results we obtained from the n-channel devices and then proceed to the p-channel results. The characteristics of the devices we tested are listed in Table 1.

Table 1: Characteristics of Devices Tested

<u>Device</u>	<u>Number of Units Tested</u>	<u>Type</u>	<u>Rated Voltage</u>	<u>Manufacturer</u>	<u>Term. Type</u>
1	3	N	150	A	F Plate
2	9	N	400	B	F Ring & F Plate
3	3	N	350	C	F Ring
4	3	N	450	C	F Ring
5	2	N	500	D	F Ring
6	2	N	1000	E	F Ring
7	2	P	150	B	F Ring
8	2	P	200	B	F Ring
9	3	P	350	C	F Ring
10	3	P	450	C	F Plate & JTE
11	3	P	350	C	JTE

N-Channel Results

The first device I tested was a 150V n-channel VD MOSFET. The initial data showed a decrease in breakdown voltage and then a partial recovery which agreed very well with the model proposed by Benedetto and Blackburn. Above about 150 krad(Si) though, the data revealed some "second order" structure that had not been reported by earlier investigators (see Figure 24), probably because most experiments collected far less data for each device. The decrease in V_{BD} , followed by a second recovery was extremely interesting since it was the first clue that there may be other phenomena contributing to the change besides the oxide trapped charge and interface states.

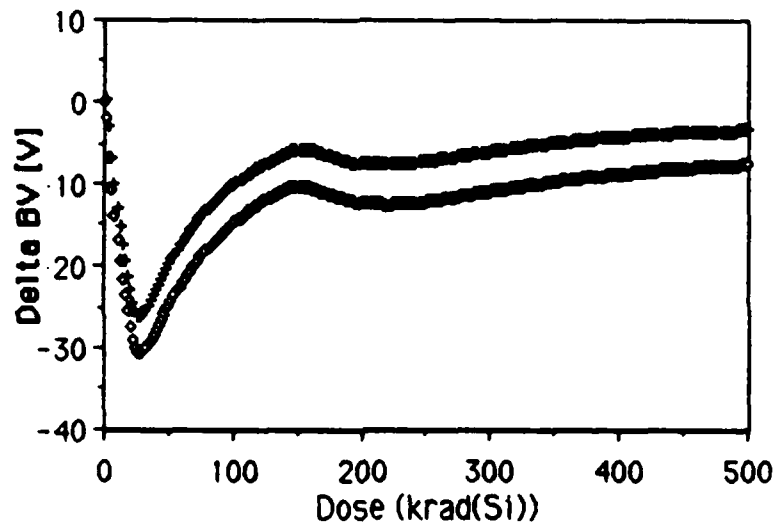


Figure 24: The Change in Breakdown Voltage During Gamma Irradiation

The results for Device 2 were inconclusive because the data varied significantly from unit to unit. After testing about 10 devices though (by far the most of any type we tested), the most frequent results were similar to those in Figure 25. This device had a combination of field plates and field rings for terminations. It was our first experience with the use of a hybrid technique: mixing more than one termination type. We later found that hybrid techniques were used frequently by manufacturers.

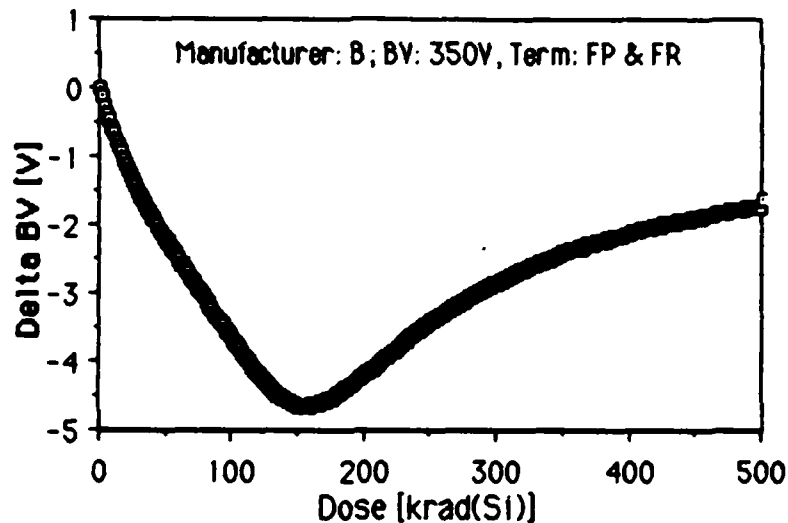


Figure 25: Breakdown Voltage Change with Increasing Dose in a 350V N-Channel

During the investigation to determine what could cause the erratic behavior between the different units when most other types of FETs were at least similar and frequently identical from unit to unit, we found that manufacturers occasionally change the termination technique used in a device from one batch to the next. For instance, someone may think that including a junction termination extension in a device that previously had only field plates may improve the breakdown voltage without increasing the cost drastically. In the next batch of devices that company makes, they may use ion implantation to include a JTE in the FET. Just as the companies are not inclined to disclose the type of termination they use in the first place, they also fail to tell circuit designers that they have modified the design of the FET. If, at some time later, the engineer that suggested the JTE feels that the improvement he expected was not attained, the termination technique used in the next batch may be the original one, or it may be another test to see if the product can be improved.

The problem with this "experimentation" by the manufacturers is that, as we will show in greater detail later, the magnitude and type of effect that radiation has on breakdown voltage is greatly dependent on the type of termination used in the device, as well as many other aspects of the

manufacturing process. If the device is tested and found to be satisfactory for use in a space satellite and at sometime later the manufacturing process is changed, even slightly, the device may no longer be acceptable in that application, but it is likely that no one knows of the change.

The next two devices tested were high voltage (350V and 450V respectively) n-channel device which had a lower power rating and used field rings as the termination technique. These two devices were very interesting because they were made by the same manufacturer, used the same field termination

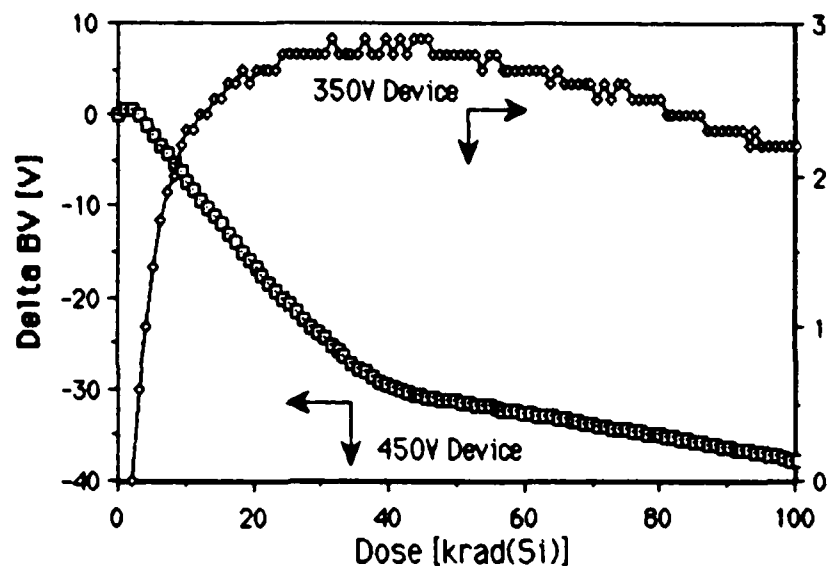


Figure 26: Breakdown Voltage of Two N-Channel FETs With Field Rings

devices, and yet had drastically different test results. As you can see in Figure 26, V_{BD} for the 350V device increased slightly during the irradiation; a result completely unexplainable with the earlier model. Although the increase was small, the result shows that there is no simple explanation for the effect of radiation on a device's breakdown voltage. The results of the 450V FET were more like the results forecasted by Benedetto's model; that is, the voltage decreased throughout the irradiation.

The next type of FET we tested was another device which responded like Benedetto had proposed after about a 20 krad dose had been accumulated;

however, it included an increase in V_{BD} initially which was not a part of Benedetto's model (see figure 27).

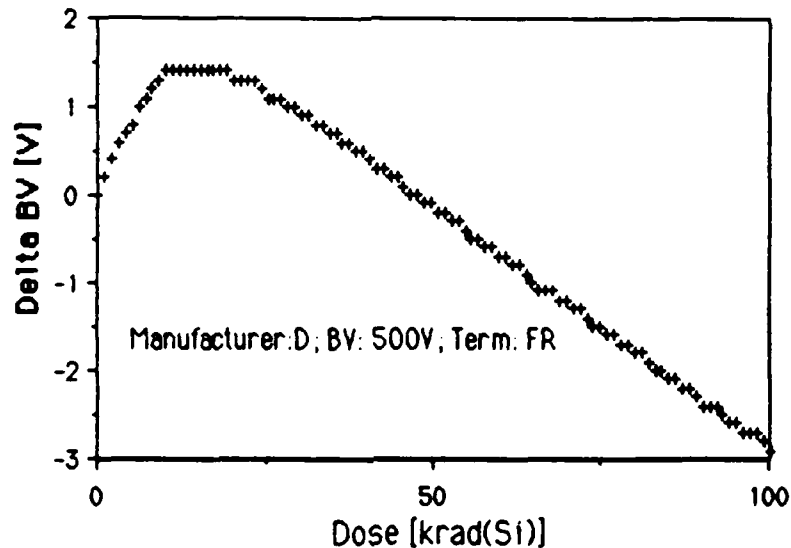


Figure 27: Breakdown Voltage of a 500V N-Channel FET

You may recall from the chapter on terminations that my analysis indicated that devices which use field rings could either increase or decrease in V_{BD} depending on whether the field rings were optimally located. The results of this experiment tend to verify those findings.

The sixth n-channel device tested was a very-high-voltage device. This device used field rings for field termination and had a manufacturers rated breakdown of 1000V. As you can see in Figure 28, the breakdown voltage of this FET decreased by one-half its manufacturers rating during the test. Although it is not shown in this figure, the starting value of this FET was approximately 1100V so that the final value was slightly greater than 500V. We never determined if this device would recover at higher doses; however, whether or not it would is not important since total circuit failure is virtually inevitable. Although this is the largest change we noted in any of our experiments, we observed almost as large a fractional change in the first p-channel FET we tested.

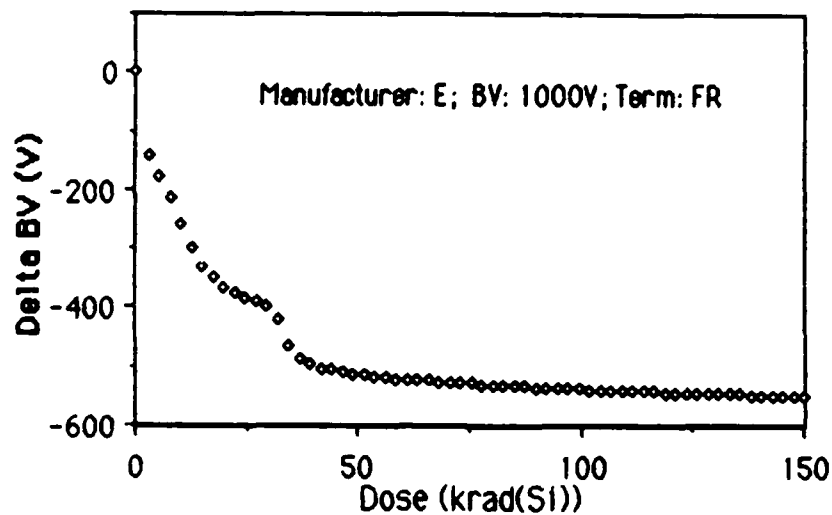


Figure 28: Results of Irradiating a Very-High-Voltage N-Channel Device

P-Channel Results

The n-channel experiments revealed information that indicated several weak points in Benedetto's model; however, the primary goal of this research was to investigate the effect of ionizing radiation on p-channel FETs. Since high-voltage p-channel FETs are a new development, no one had investigated the effect of radiation on them yet. We had some difficulty obtaining parts to test since, being a new development, p-channel power MOSFETs are not widely used. After obtaining four types of p-channel FETs we modified the test set to accept p-channel devices and began testing. By the luck of the draw, the first p-channel device we tested was in many ways the most interesting of all.

The first p-channel device was rated at 450V and used a narrow field plate and a JTE for field termination. Although we expected the device to increase in breakdown voltage with increasing dose, it promptly decreased from a little above 550V to 510V then rapidly recovered to slightly above the original value as shown in Figure 29. It then decreased slightly and then started increasing with increasing dose. We were surprised by these results. In fact, it is

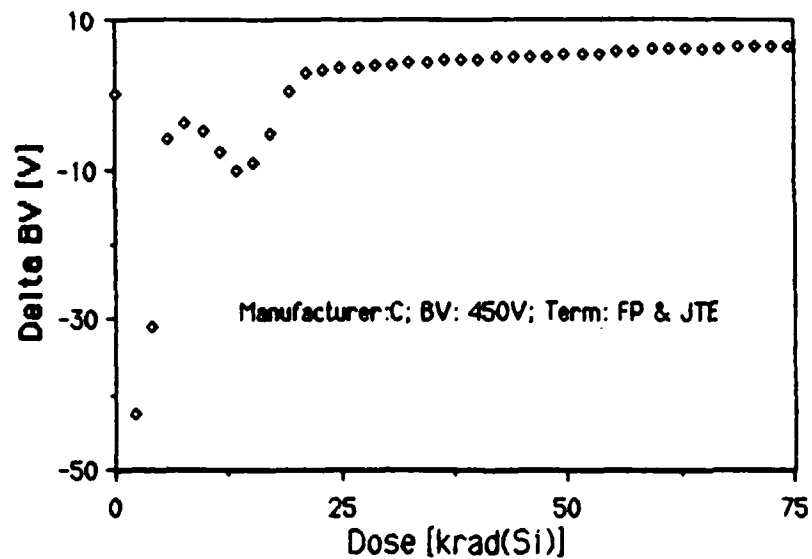


Figure 29: Change in P-Channel Breakdown Voltage During Gamma Irradiation

possible that the maximum change in breakdown voltage was greater than the maximum value shown above. The reason is that we expected more gradual changes and were making measurements about every 2500 rad(Si). The next time we tested this device type we made more frequent measurements and observed about a 125V change in breakdown voltage (see figure 30).

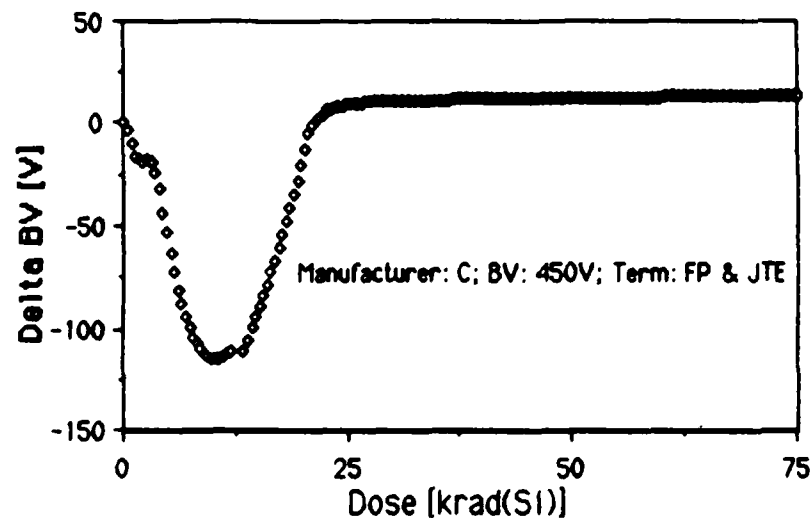


Figure 30: Change in P-Channel Breakdown Voltage During Gamma Irradiation

These results are significant for several reasons. Some n-channel results indicated that the mechanisms which cause the change in breakdown voltage are more complicated than those proposed earlier. This was, however, the first time we had obtained data that was contrary to what had been proposed. Second, but far more important, is that many designers expect any significant changes in breakdown voltage to occur after exposures over about 50 krad(Si). Therefore, it is possible that devices would not be tested at such low levels. Thus based on current expectations of radiation damage. If the devices had been tested at this dose level and had been tested using what I called a "typical procedure", it is possible that the prompt drop in breakdown voltage would have been missed. Finally, this shows that circuits which are exposed to relatively low doses of ionizing radiation may be susceptible to radiation damage.

The next device tested was made by the same manufacturer but used field ring field terminations. The results for this device epitomized those anticipated by Benedetto's model. The breakdown voltage of the device increased with increasing dose, although it was beginning to decrease at the end of the experiment as shown in Figure 31. This is in agreement with the

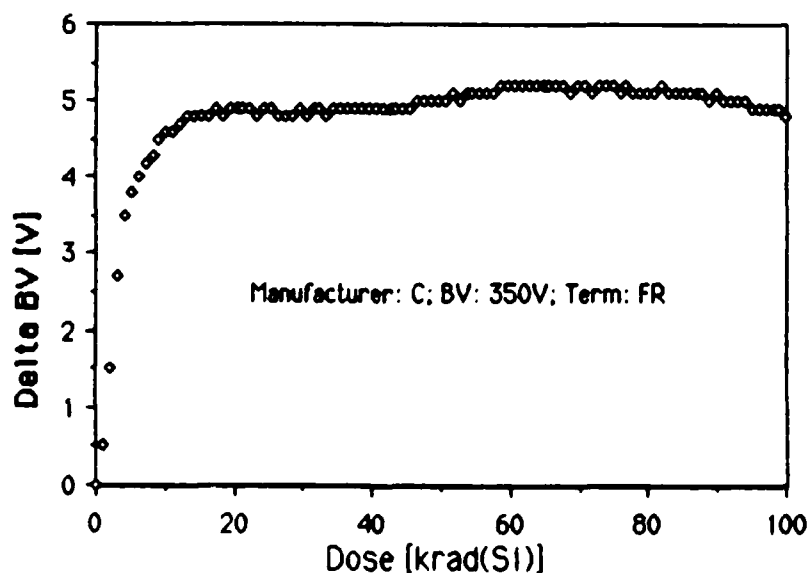


Figure 31: Change in Breakdown Voltage of a Moderate Voltage P-Channel FET

analysis of field rings presented in the chapter on terminations. The increase is a result of the radiation improving the optimization of the field ring. When the ring is optimized, further irradiation causes the breakdown voltage to decrease.

Another device of the same type provided even further verification of the behavior I expected in field ring devices. Notice in Figure 32 that the breakdown voltage first increases, then decreases, and then increases again. This behavior can be attributed to the fact that this device has several field rings. At the beginning of the irradiation, increasing gamma dose improves the performance of one of the rings, and then, after obtaining the optimum for that ring, the breakdown begins decreasing with increasing dose. At some point, about 50 krad in Figure 32, the optimization of another ring begins to influence the breakdown voltage change. This is reasonable, in fact expected, since there is no reason to believe that it would take the same amount of radiation to optimize all of the field rings.

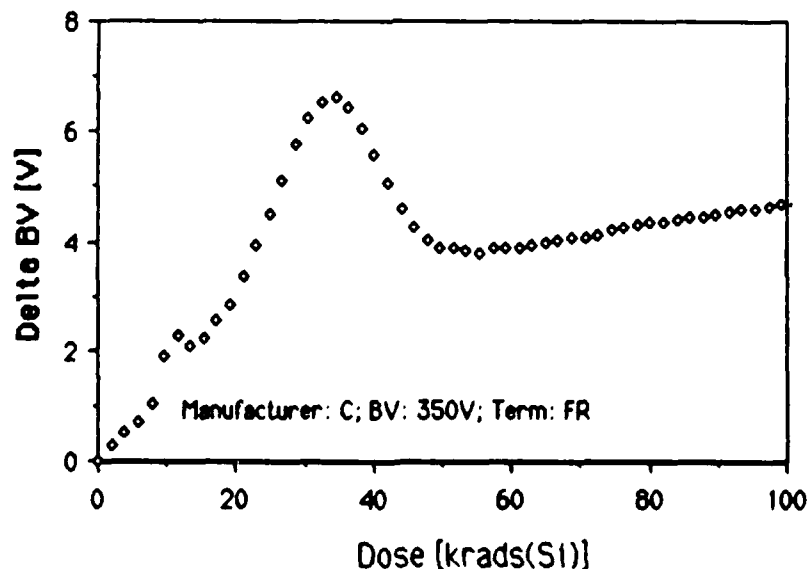


Figure 32: Results for Another Moderate Voltage P-Channel FET

Another important feature depicted in these two figures (31 and 32) is that for lower voltage devices, the change in breakdown voltage is less than the changes found in higher voltage devices. This is because the termination technique is not providing as much improvement in lower voltage devices; therefore, the results of removing the termination is not as severe. This feature was also noted in the next device tested.

The last device was a low voltage p-channel MOSFET which used field rings for electric field termination (see Figure 33). Note that the correspondence between low voltage rating and small change in breakdown voltage is shown. In order for results to agree with the field ring analysis though, the breakdown voltage would have to start decreasing. The other experiments indicate that it is unlikely that there would be any significant changes in the character of the results above 500 krad.

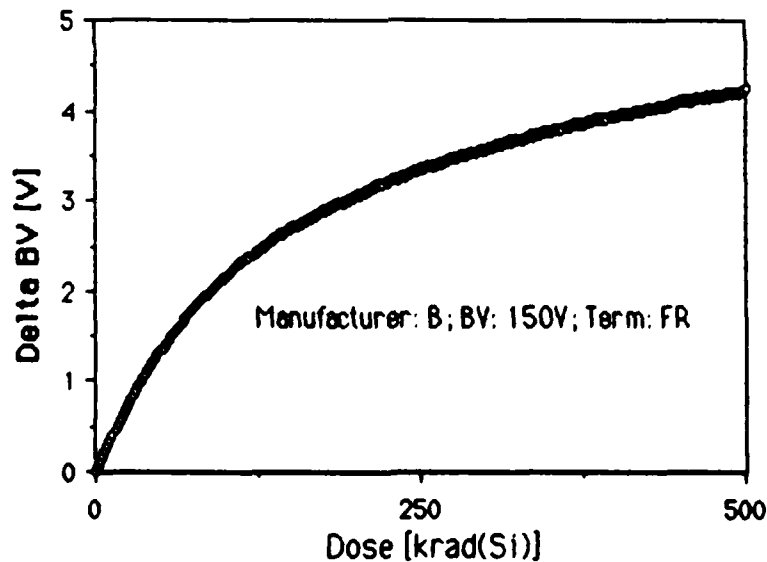


Figure 33: Change In Breakdown Voltage for Low Voltage P-Channel MOSFET

CHAPTER 8

CONCLUSIONS

The original purpose of this experiment was to evaluate the model presented by Benedetto for radiation-induced change in V_{BD} for p-channel MOSFETs. Benedetto had proposed that the V_{BD} changes were determined by the type of termination used in the device and that one could expect an increase in breakdown voltage for p-channel devices. I found that this model could not account for the observed behavior; however, the differences could usually be attributed to differences in the type of field terminations.

The analysis of field termination theory indicates that there is a maximum V_{BD} that can be obtained by using any field termination. That maximum is roughly twice the V_{BD} of the same device without any terminations. The maximum affect of radiation is to cancel the effect of the termination, therefore the maximum change in V_{BD} one would expect to see would be a decrease to one-half the original value. That result was observed in Device 5 (see Table 1).

The termination theory also indicates that the termination technique plays a much more important role in higher voltage devices. That is, the in V_{BD} improvement caused by using the termination technique is greater in high-voltage devices than it is in low-voltage devices. Thus one would expect the amount of change in V_{BD} to increase with increasing voltage ratings. That tendency was also observed; thus the theory presented in earlier chapters is born out by the results of the experiments. This indicates that in low voltage devices, regardless of the type of termination is used, the radiation-induced changes in V_{BD} will be small.

The field termination theory indicates that in p-channel devices one can expect either an increase in V_{BD} depending on the type of termination used. The results indicate that p-channel devices which use only field plate terminations and have a pure field oxide will generally show an increase in V_B .

The p-channel MOSFETs which only use only junction termination extensions and have high-quality oxides will generally exhibit a decrease in V_{BD} with increasing dose. In all cases, larger decreases were observed in higher voltage devices.

Experiments on both n- and p-channel devices with field ring terminations showed that there is no way to predict the low dose effects on V_{BD} . This is because of the results of irradiating the device will strongly depend on how well the field rings had been optimized. Since the level of optimization depends on how accurately the rings are located and since the location of the rings is an extremely difficult parameter to calculate, frequently irradiation improves the effect of the rings, thereby improving the breakdown voltage. After exposure to a large dose, field ring terminated devices usually exhibit a decrease in V_{BD} .

N-channel devices with either field plates or JTEs will generally decrease in breakdown voltage. Devices with field plate terminations will generally decrease and then show some recovery toward the original V_{BD} values without ever achieving complete recovery. Units using only a JTE for termination will always decrease in V_{BD} . In general, field rings seem to show the smallest change in intermediate voltage devices. The problem with these "models" is that frequently manufacturers include two termination types in a device so that none of the "simple models" accurately predict the results of irradiation.

Another important point revealed in this research is the existence of second order effects which are not covered by the field termination theory. Subsequent literature research indicates that other device features, especially characteristics of the oxide covering the field region of the device, can have an impact on breakdown voltage. It is reasonable to assume that these features also modify the device response to radiation; however, further research is required in this area.

The experimental results also pointed out the need for measurements of V_{BD} at frequent dose intervals as done in the experiments in this research. It

is easy to see in the results reported in the last chapter that by measuring several devices of the same type at only a few dose levels and then averaging the results for each device, many significant characteristics of the device can be lost. By taking data points at frequent dose intervals, each data set can be analyzed independently without introducing significant error. This allows analysis of the types of changes observed in the 450V p-channel device which would be lost if the results had been averaged together. The large number of data points will also point out the rapid changes and recovery observed in that device. Without the frequent measurements, these types of changes could be completely missed.

REFERENCES

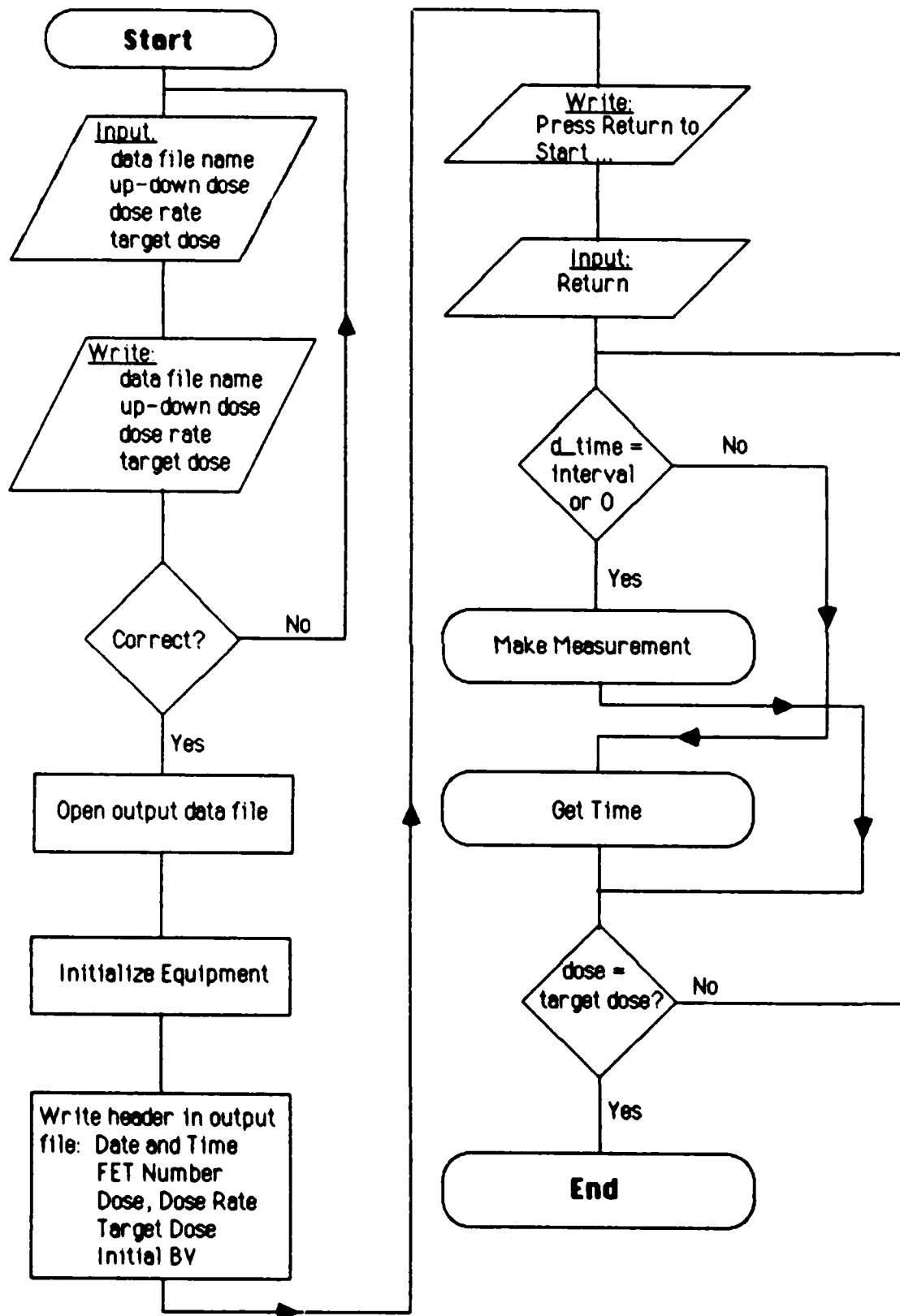
1. Data Book, Supertex Inc., Sunnyvale, CA (1984).
2. F.B. McLean, H.E. Boesch Jr., and J.M. McGarrity, "Hole Transport and Recovery of SiO₂ Gate Insulators", IEEE Trans. Nucl. Sci., NS-23, 1506 (1976).
3. P.S. Winoker and H.E. Boesch Jr., "Interface State Generation in Radiation Hard Oxides", IEEE Trans. Nucl. Sci., NS-27, 1647 (1980).
4. J.R. Schwank, et al., "Physical Mechanisms Contributing to Device Rebound", IEEE Trans. Nucl. Sci., NS-31, 1737 (1984).
5. J.M. McGarrity "Considerations for Hardening MOS Devices and Circuits for Low Radiation Doses", IEEE Trans. Nucl. Sci., NS-27, 1739 (1980).
6. G.F. Derbenwick, and B.L. Gregory, "Process Optimization of Radiation Hardened CMOS Integrated Circuits", IEEE Trans. Nucl. Sci., NS-22, 2151 (1975).
7. J.M. Benedetto, The Effect of Ionizing Radiation on the Breakdown Voltage of Power MOSFETs, MSEE Thesis, Electrical Engineering Department, University of Maryland, College Park, MD, Aug 1983.
8. A.S. Grove, Physics and Technology of Semiconductor Devices, John Wiley and Sons, New York, (1967).
4. R.M. Warner, and B.L. Grung, Transistors, John Wiley and Sons, New York, (1983).
9. R.J. Smith, Circuits, Devices, and Systems, John Wiley and Sons, New York, (1984).
10. S.K. Ghandhi, Semiconductor Power Devices, John Wiley and Sons, New York, (1977).
11. D.G. Ong, Modern MOS Technology, McGraw Hill, New York, (1984).
12. P. Richman, MOS Field-Effect Transistors and Integrated Circuits, McGraw-Hill, New York, (1973).
13. HEXFET Data Book, International Rectifier, El Segundo, CA (1982-1983).
14. B.J. Baliga, "High-voltage Device Termination Techniques. A comparative review", IEE Proceedings, 129, 173, (1982). [British Journal]
15. K.P. Brieger, W. Gerlach, and J. Pleka, "Blocking Capability of Planar Devices with Field Limiting Rings", Solid State Electronics, 26, 739, (1983)

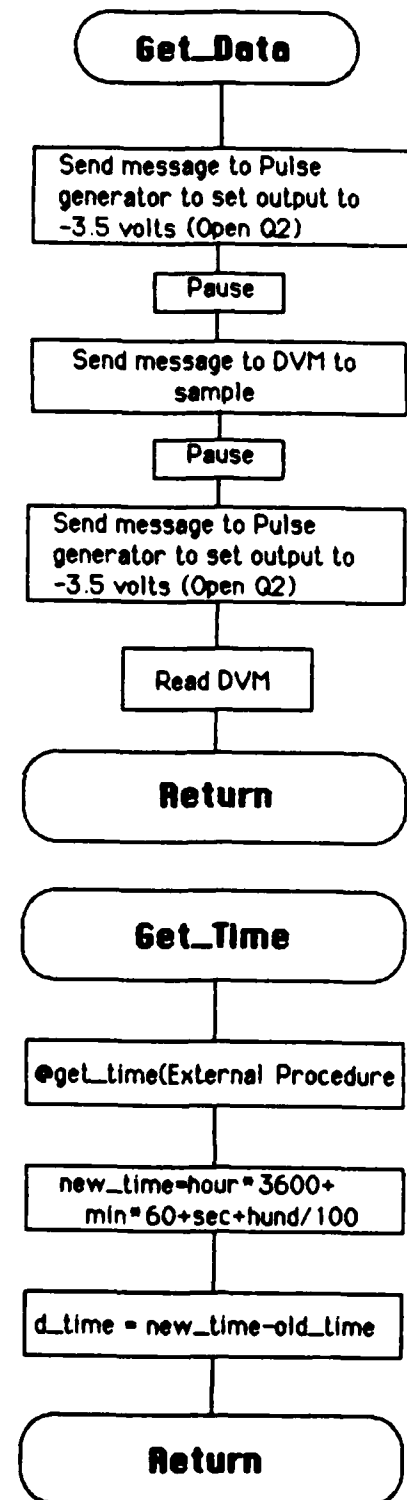
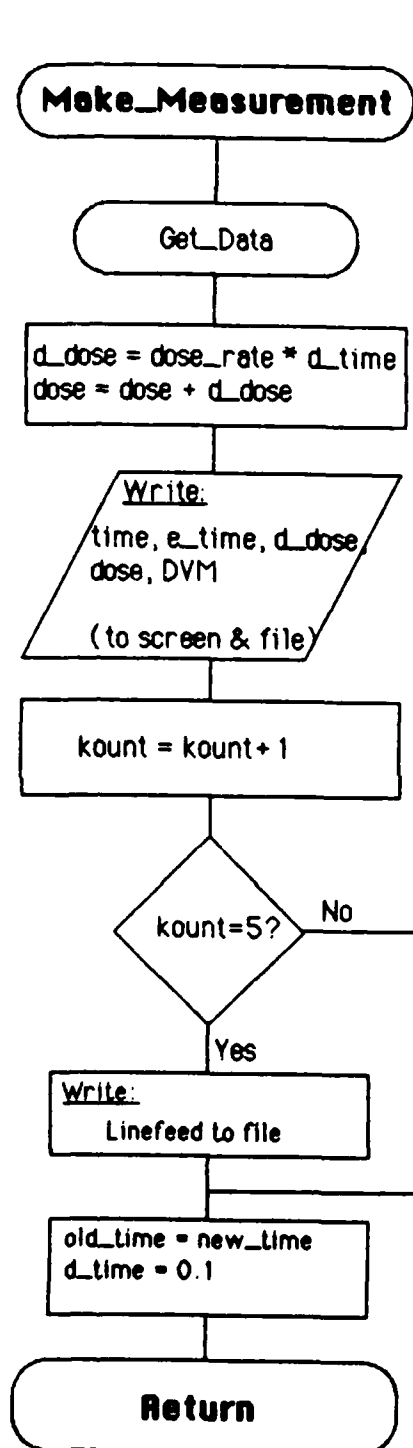
16. D.L. Blackburn, J.M. Benedetto, and K.F. Galloway, "The Effect of Ionizing Radiation on the Breakdown Voltage of Power MOSFETs", IEEE Trans. on Nucl. Sci., NS-30, 4116, (1983).
17. R.D. Pugh, A.H. Johnston, and K.F. Galloway, "Characteristics of the Breakdown Voltage of Power MOSFETs After Total Dose Irradiation", to be published.

APPENDIX A
COOLDOWN
A PASCAL PROGRAM TO EVALUATE MOSFET BREAKDOWN VOLTAGE

The COOLDOWN program was designed and written to operate the test equipment and record the data necessary to evaluate the effect of radiation on the breakdown voltage of power MOSFETs. COOLDOWN, a new version of the original program FETRAD which was also developed for this research project, added the ability to measure the effect of annealing on the breakdown voltage. In addition, a copy of the FORTRAN program RERITE, a program to convert the COOLDOWN output into an input for the commercial program Cricket Graph, is included.

The flow chart for the main program is on page 64 and the flow charts for the major procedures (subroutines) are on page 65. The source code for the COOLDOWN program starts on page 66 and RERITE begins on page 73.





PROGRAM cooldown;

```
(* PROGRAM:          COOLDOWN ( A modified version of FETRAD )
   WRITTEN BY:        Bob Pugh
   DATE:              1 FEB 1986
```

The COOLDOWN version of FETRAD performs the normal FETRAD functions described below and also allows the test to continue after the irradiation has been terminated to measure the effects of "room temperature" annealing.

```
PROGRAM:          FETRAD
WRITTEN BY:        Bob Pugh
DATE:              14 DEC 1986
```

This program runs an experiment to measure the change in breakdown voltage of power MOSFETS as they are irradiated in a Gammacell. It runs on an IBM PC with an IEEE 488 bus card installed. The PC is connected via the bus to an HP 8112 Pulse Generator and a Keithely 175/197 DMM. The program changes the output state on the pulse generator, samples the DMM, returns the pulse generator output to its nominal state, calculates the dose increment for the measurement period, calculates the total dose, and writes all the pertinent data to a disk file. The program uses several non-standard external subroutines. *

```
CONST
  space      = ' ';
  colon      = ':';
  dma_adr    = '11';
  fgndr      = '4';

VAR
  file_name  : string[15];
  fet_data   : text;
  interval   : real;
  dose_rate, max_dose : real;
  dose, d_dose, up_down : real;
  dma_out    : real;
  i, kount   : integer;
  msg, crlf  : string;
  time, date : string;
  d_time, e_time, f_time : real; { delta, elapse, and first times}
  old_time, new_time : real;
  c_time, cool_down : real;
  dummy      : string;
```

```
EXTERNAL PROCEDURE bus_on;
EXTERNAL PROCEDURE bus_off;
EXTERNAL PROCEDURE remote( adr : string);
EXTERNAL PROCEDURE local( adr : string);
EXTERNAL PROCEDURE dev_clr( adr : string);
EXTERNAL PROCEDURE send_str( adr, msg : string);
```

```

EXTERNAL PROCEDURE recu_str( adr : string; var msg : string);
EXTERNAL PROCEDURE trigger( adr : string);
EXTERNAL PROCEDURE set_terminators( term : string);
EXTERNAL PROCEDURE @gettime( VAR hour, min, sec, hund : integer);
EXTERNAL PROCEDURE @getdate( VAR month, day, year : integer);
EXTERNAL PROCEDURE @hit;
EXTERNAL PROCEDURE num_to_str( n:real; format:char; dec:integer; VAR
    x:string);
EXTERNAL FUNCTION sq_status:boolean;
EXTERNAL FUNCTION str_to_real( msg : string) : real;

```

```

{ ----- }

```

```

PROCEDURE intro;

```

```

    VAR

```

```

        f_name          :string[9];
        drive            :string[2];

```

```

    BEGIN

```

```

        writeln(' This program is designed to operate an experiment to ');
        writeln(' measure the effects of gamma radiation on Power MOSFETS');
        writeln(' Before the experiment can begin, you must provide the ');
        writeln(' experimental parameters. ');
        writeln;
        writeln;
        write(' First, enter the name of the output data file: ');
        read (f_name);
        writeln;
        write(' Which drive do you want that file written to: ');
        read (drive);
        writeln;
        filename := concat (drive, colon, f_name, '.DAT');
        write(' Next, enter the up-down dose for this experiment (in RADS):
            ');
        read (up_down);
        writeln;
        write(' Now enter the dose rate the FET will receive (in RADS/SEC):
            ');
        read (dose_rate);
        writeln;
        write(' This time enter the time interval between measurements (in
            SEC): ');
        read (interval);
        writeln;
        write(' Enter the total dose target (in RADS): ');
        read (max_dose);
        writeln;
        write(' Finally, enter the cool down time (in seconds): ');
        read (cool_down);
        writeln;
        verify;
    END; (intro)

```

```

{ ----- }

```

```
PROCEDURE verify;  
BEGIN
```

```

writeln;
writeln;
writeln;
writeln('    Is the following data correct?');
writeln;
writeln('        OUTPUT FILENAME:                ',file_name);
writeln('        UP-DOWN DOSE:                        ',up_down:5:1,' rads');
writeln('        DOSE RATE:                            ',dose_rate:6:1,'
    rads/sec');
writeln('        MEASUREMENT INTERVAL:                ',interval:4:0,' sec');
writeln('        FINAL DOSE:                          ',max_dose:7:0,' rads');
writeln('        COOL DOWN TIME:                      ',cool_down:7:0,' sec');
writeln;
writeln;
write(' Enter Y or N -> ');
read(dummy);
writeln;
IF ( DUMMY[1] <> 'Y') and ( DUMMY[1] <> 'y')then intro;
END;
```

```
PROCEDURE open_file;
```

```
BEGIN
  assign(fet_data,file_name);
  rewrite(fet_data);
  if ioreult = 255 then
    BEGIN
      writeln(' There was an error opening the output file. PROGRAM
        ABORTED!!');
      @hit
    END;
END;
```

$$\{ \text{-----} \}$$

```
PROCEDURE header;
```

```
BEGIN
  get_date;
  get_time;
  writeln (fet_data);
  writeln (fet_data);
  writeln (fet_data, '
    file_name);
  writeln (fet_data);
  writeln (fet_data, '
  DATE: ', date);
  writeln (fet_data, '
  TIME: ', time);
  writeln (fet_data);
  get_data;
  writeln (fet_data, '
    msg);
  writeln (fet_data);
  writeln (fet_data, '
  INITIAL (unirradiated) BREAKDOWN VOLTAGE: ',
  EXPERIMENT PARAMETERS:');

```

```

writein (fet_data, '
rads');
writein (fet_data, '
rads/sec');
writein (fet_data, '
sec');
writein (fet_data, '
rads');
writein (fet_data, '
sec');
writein (fet_data);
writein (fet_data);
writein (fet_data,
=====');

```

```

writein (fet_data);
writein (fet_data, '
DUM');
writein (fet_data, '
READING');
writein (fet_data);
END; (header)

(-----)

```

TIME		DOSE	
CLOCK	ELAPSE	DELTA	TOTAL

PROCEDURE initializ_equip;

CONST

```

dva_msg      = 'R5 T5 M9 G1 ';
fgn_msg      = 'M2,W1,L0,C1,D0,PER 500 MS,WID 200 MS,HIL
5.00U,LOL -3.57U';
(M2,T1,W4,WID90MS,AMP5.0U)

```

BEGIN

```

writein(' The program expects to be connected to a Keithly DMM (A 11)
and');
writein(' on HP 8112 Pulse Generator (A 4) via the GPIB. Ensure all
the');
write(' equipment is properly configured (turned on) then press
<RETURN>');
readin( dummy ); writein; writein;
bus_on;
remote( dva_adr);
remote( fgn_adr);
CrLf := concat(chr(13),chr(10));
set_terminators(CrLf);
dev_clr( dva_adr);
dev_clr( fgn_adr);
msg := concat(dva_msg, CrLf);
send_str( dva_adr, dva_msg);
msg := concat(fgn_msg, CrLf);
send_str( fgn_adr, msg);
END; (initializ_equip)

```

(-----)

PROCEDURE get_date;


```
CONST
    names          = 'JANFEBMARAPRIMAYJUNJULUGSEP OCTNOVDEC';
```

```
VAR
    day, month, year : integer;
    temp1, temp2      : string;
```

```
BEGIN
    @get_date(month, day, year);
    num_to_str(day, '1', 2, temp1);
    temp2 := copy(names, 3*month-2, 3);
    temp1 := concat(temp1, ' ', temp2);
    num_to_str(year, '1', 4, temp2);
    date := concat(temp1, ' ', temp2);
END; (get_date)
```

```
{-----}
```

```
PROCEDURE get_time;
```

```
CONST
    sec_per_hour      = 3600;
    sec_per_min       = 60;
```

```
VAR
    hour, min, sec, hund : integer;
    hour_st, min_st, sec_st : string;
```

```
BEGIN
    @gettime( hour, min, sec, hund );
    new_time := (hour * sec_per_hour) + (min * sec_per_min) + sec + hund/100;
    d_time := new_time - old_time;
```

```
IF (d_time < 0) THEN
    BEGIN
        d_time := (new_time + 2400 - old_time);
        f_time := -e_time;
    END;
```

```
e_time := new_time - f_time;
num_to_str(hour, '1', 2, hour_st);
if (length(hour_st) = 1) then hour_st := concat('0', hour_st);
num_to_str(min, '1', 2, min_st);
if (length(min_st) = 1) then min_st := concat('0', min_st);
num_to_str(sec, '1', 2, sec_st);
if (length(sec_st) = 1) then sec_st := concat('0', sec_st);
time := concat(hour_st, colon, min_st, colon, sec_st);
END; (get_time)
```

```
{-----}
```

```
PROCEDURE get_data;
```

```
VAR
    i, x          : integer;
    temp_str      : string;
```

```
BEGIN
    msg := concat('CO', crlf);
```

```

send_str(fgn_adr, msg);
for i := 0 to 30000 do x := i;
msg := concat('X', chr(i));
send_str(dva_adr, msg);
for i := 0 to 25000 do x := i;
msg := concat('C1', chr(i));
send_str(fgn_adr, msg);
recv_str(dva_adr, msg);
temp_str := copy(msg, 1, length(msg)-2);
dva_out := str_to_real(temp_str);
END; {get_data}

```

(-----)

PROCEDURE wake_measurement;

```

CONST
    sp3          = ' ';
    sp5          = ' ';

BEGIN
    get_data;
    d_dose := dose_rate * d_time ;
    dose := dose + d_dose;
    writeln(fet_data, sp5, time, sp5, e_time:7:1, sp3, d_dose:6:2, sp5, dose:7:0,
        sp3, dva_out:7:2);
    writeln(sp5, time, sp5, e_time:7:1, sp3, d_dose:6:2, sp5, dose:7:0,
        sp3, dva_out:7:2);
    kount := kount + 1;
    if kount >= 5 then
        BEGIN
            writeln(fet_data);
            writeln;
            kount := 0;
        END;
    old_time := new_time;
    d_time := 0.1;
END; {wake_measurement}

```

(-----)

PROCEDURE all_done;

```

BEGIN
    local(dva_adr);
    local(fgn_adr);
    CLOSE (fet_data, i);
    if (i <> 0) then writeln(' THERE WAS AN ERROR CLOSING THE OUTPUT
        FILE!!!');
    END;

```

(=====)

BEGIN

```

    intro;
    writeln(' Now that we have the necessary info, the experiment will

```

```

begin.'');

open_file;
initializ_equip;
header;

writeln(' Press <RETURN> when the device is at the bottom of the well. ');
kount := 0;
dose := up_down/2.0;
old_time := 36000;
readln( dummy );
get_time;
d_time := 0;
e_time := 0;
f_time := new_time;

REPEAT
  IF (d_time <= 0 ) or ( d_time >= interval) THEN
    make_measurement
  ELSE
    get_time
  UNTIL (dose >= max_dose);

IF (cool_down > 0.0 ) THEN
  BEGIN
    get_time;
    c_time := e_time;
    interval := cool_down / 100;
    dose_rate := 0.0;

    REPEAT
      IF (d_time >= interval) THEN
        make_measurement
      ELSE
        get_time
    UNTIL ((e_time - c_time) >= cool_down);
  END; {IF}

all_done;
END. {cooldown}

```

PROGRAM RERITE

```

C
C   This program reads an output file from the COOLDOWN program and
C   converts it to an input file for Cricket Graph. This program
C   is written to run on a Macintosh Plus. A Cricket input
C   file must have the data columns separated by TAB characters.
C   The only data from COOLDOWN used are the elapse time, the total
C   dose, and the DUM reading.
C
C   CHARACTER STRING*80, TAB, FNAME*9, ANS
C   TAB=CHAR(9)
C   4  FORMAT(A1)
C   5  FORMAT(15X,F10.1,20X,F7.0,8X,F7.2)
C   6  FORMAT(10X,F10.1,A1,F7.0,A1,F7.2)
C   7  FORMAT(A20)
C   8  FORMAT('  ENTER INPUT FILENAME')
C   9  FORMAT('  ENTER OUTPUT FILENAME')
C
C   Enter input file name and open file
C
C   10 WRITE(*,8)
C      READ(*,7) FNAME
C      OPEN (UNIT=2,STATUS='OLD',FILE=FNAME)
C
C   Enter output file name and open file
C
C      WRITE(*,9)
C      READ(*,7) FNAME
C      OPEN (UNIT=3,STATUS='NEW',FILE=FNAME)
C
C   First 23 lines of COOLDOWN file is the header; therefore skip over
C
C      DO 20 I=1,23
C          READ(2,7) STRING
C   20  CONTINUE
C      WRITE(*,7)' Working...'
C
C   Read input file and write to output file. Repeat for five lines
C   skip blank line and jump back to do loop. Repeat until end of file
C
C   25 DO 30 I=1,5
C       READ(2,5,END=35) X1, X2, X3
C       WRITE(3,6) X1,TAB,X2,TAB,X3
C   30  CONTINUE
C       READ(2,7,END=35) STRING
C       GO TO 25
C
C   Find out if user wants to run another input file
C
C   35 WRITE(*,*)' Would you like to process another file (Y/N)?'
C      READ(*,4) ANS
C      IF((ANS.EQ.'Y').OR.(ANS.EQ.'y')) GOTO 10
C      STOP
C      END

```

APPENDIX B
A REPRESENTATIVE DATA FILE

This Appendix contains one data file which shows the form and content of a result file from one experiment. It is from an experiment on a device type 1 (see Table 1, page 48).

RESULTS OF EXPERIMENT C: IR241_1.DAT

DATE: 27 JAN 1986

TIME: 09:12:47

INITIAL (unirradiated) BREAKDOWN VOLTAGE: +0.23780E+3

EXPERIMENT PARAMETERS:

UP-DOWN DOSE: 408.0 rads
 DOSE RATE: 80.6 rads/sec
 MEASUREMENT INTERVAL: 25. sec
 TARGET DOSE: 500000. rads

```
=====
```

----- TIME -----		----- DOSE -----		DUM READING
CLOCK	ELAPSE	DELTA	TOTAL	
09:13:11	0.0	0.00	204.	237.75
09:13:36	25.0	2018.22	2222.	235.79
09:14:01	50.1	2019.03	4241.	230.85
09:14:26	75.1	2018.22	6259.	226.97
09:14:51	100.2	2019.03	8279.	223.77
09:15:16	125.2	2019.03	10298.	220.99
09:15:41	150.3	2018.22	12316.	218.50
09:16:06	175.3	2019.03	14335.	216.22
09:16:31	200.4	2023.06	16358.	214.13
09:16:56	225.5	2018.22	18376.	212.18
09:17:21	250.5	2015.00	20391.	210.41
09:17:46	275.5	2018.22	22409.	208.87
09:18:11	300.5	2019.03	24428.	207.72
09:18:36	325.6	2018.22	26447.	207.13
09:19:01	350.6	2015.00	28462.	207.04
09:19:26	375.6	2018.22	30480.	207.29
09:19:51	400.7	2019.03	32499.	207.73
09:20:17	425.7	2018.22	34517.	208.26
09:20:42	450.8	2019.03	36536.	208.86
09:21:07	475.8	2019.03	38555.	209.44
09:21:32	500.9	2018.22	40573.	210.06
09:21:57	525.9	2019.03	42592.	210.67
09:22:22	551.0	2018.22	44611.	211.27
09:22:47	576.0	2019.03	46630.	211.87
09:23:12	601.0	2019.03	48649.	212.48

09:23:37	626.1	2018.22	50667.	213.06
09:24:02	651.1	2019.03	52686.	213.66
09:24:27	676.2	2018.22	54704.	214.18
09:24:52	701.2	2019.03	56723.	214.72
09:25:17	726.3	2019.03	58742.	215.24
09:25:42	751.3	2018.22	60760.	215.77
09:26:07	776.4	2019.03	62779.	216.27
09:26:32	801.4	2018.22	64798.	216.75
09:26:57	826.5	2019.03	66817.	217.23
09:27:22	851.5	2019.03	68836.	217.66
09:27:47	876.6	2023.06	70859.	218.09
09:28:12	901.6	2018.22	72877.	218.52
09:28:38	926.7	2019.03	74896.	218.92
09:29:03	951.7	2018.22	76914.	219.32
09:29:28	976.7	2015.00	78929.	219.69
09:29:53	1001.8	2023.06	80952.	220.06
09:30:18	1026.9	2023.06	82975.	220.43
09:30:43	1052.0	2018.22	84994.	220.77
09:31:08	1077.0	2019.03	87013.	221.11
09:31:33	1102.1	2019.03	89032.	221.44
09:31:58	1127.1	2018.22	91050.	221.76
09:32:23	1152.2	2019.03	93069.	222.06
09:32:48	1177.2	2018.22	95087.	222.35
09:33:13	1202.3	2019.03	97106.	222.64
09:33:38	1227.3	2019.03	99125.	222.93
09:34:03	1252.3	2018.22	101143.	223.19
09:34:28	1277.5	2023.06	103166.	223.44
09:34:53	1302.5	2019.03	105185.	223.69
09:35:18	1327.5	2018.22	107204.	223.95
09:35:43	1352.5	2015.00	109219.	224.18
09:36:08	1377.6	2018.22	111237.	224.41
09:36:33	1402.6	2019.03	113256.	224.67
09:36:58	1427.7	2018.22	115274.	224.86
09:37:23	1452.7	2015.00	117289.	225.09
09:37:49	1477.7	2018.22	119307.	225.28
09:38:14	1502.8	2023.06	121330.	225.49
09:38:39	1527.9	2019.03	123350.	225.66
09:39:04	1553.0	2023.06	125373.	225.87
09:39:29	1578.0	2019.03	127392.	226.06
09:39:54	1603.0	2018.22	129410.	226.24
09:40:19	1628.1	2019.03	131429.	226.42
09:40:44	1653.1	2018.22	133447.	226.62
09:41:09	1678.2	2019.03	135466.	226.76

09:41:34	1703.3	2023.06	137489.	226.93
09:41:59	1726.3	2019.03	139508.	227.09
09:42:24	1753.4	2018.22	141526.	227.26
09:42:49	1778.4	2019.03	143545.	227.40
09:43:14	1803.5	2018.22	145564.	227.50
09:43:39	1828.5	2019.03	147583.	227.55
09:44:04	1853.6	2019.03	149602.	227.58
09:44:29	1878.6	2018.22	151620.	227.56
09:44:54	1903.7	2019.03	153639.	227.56
09:45:20	1928.7	2018.22	155657.	227.52
09:45:45	1953.7	2015.00	157672.	227.45
09:46:10	1978.7	2018.22	159690.	227.35
09:46:35	2003.8	2019.03	161709.	227.23
09:47:00	2028.8	2018.22	163728.	227.10
09:47:25	2053.9	2019.03	165747.	227.00
09:47:50	2079.0	2023.06	167770.	226.88
09:48:15	2104.0	2019.03	169789.	226.77
09:48:40	2129.1	2018.22	171807.	226.66
09:49:05	2154.1	2019.03	173826.	226.58
09:49:30	2179.2	2018.22	175844.	226.46
09:49:55	2204.2	2015.00	177859.	226.35
09:50:20	2229.2	2018.22	179878.	226.27
09:50:45	2254.3	2019.03	181897.	226.17
09:51:10	2279.3	2018.22	183915.	226.08
09:51:35	2304.3	2019.03	185934.	226.01
09:52:00	2329.4	2019.03	187953.	225.92
09:52:25	2354.4	2018.22	189971.	225.85
09:52:50	2379.5	2019.03	191990.	225.78
09:53:15	2404.5	2018.22	194008.	225.71
09:53:40	2429.5	2015.00	196023.	225.65
09:54:05	2454.6	2018.22	198042.	225.60
09:54:30	2479.6	2019.03	200061.	225.55
09:54:55	2504.6	2018.22	202079.	225.50
09:55:21	2529.7	2019.03	204098.	225.47
09:55:46	2554.8	2019.03	206117.	225.44
09:56:11	2579.8	2018.22	208135.	225.41
09:56:36	2604.8	2019.03	210154.	225.38
09:57:01	2629.9	2018.22	212172.	225.36
09:57:26	2654.9	2019.03	214191.	225.34
09:57:51	2680.0	2019.03	216210.	225.34
09:58:16	2705.0	2018.22	218229.	225.33
09:58:41	2730.1	2019.03	220248.	225.33
09:59:06	2755.1	2018.22	222266.	225.33

09:59:31	2780.2	2019.03	224285.	225.34
09:59:56	2805.3	2023.06	226308.	225.34
10:00:21	2830.3	2019.03	228327.	225.36
10:00:46	2855.3	2018.22	230345.	225.37
10:01:11	2880.4	2019.03	232364.	225.39
10:01:36	2905.4	2018.22	234382.	225.41
10:02:01	2930.4	2015.00	236397.	225.45
10:02:26	2955.5	2018.22	238416.	225.47
10:02:51	2980.5	2019.03	240435.	225.50
10:03:16	3005.6	2018.22	242453.	225.54
10:03:41	3030.6	2019.03	244472.	225.57
10:04:06	3055.7	2019.03	246491.	225.60
10:04:32	3080.7	2018.22	248509.	225.64
10:04:57	3105.8	2019.03	250528.	225.68
10:05:22	3130.8	2018.22	252546.	225.73
10:05:47	3155.8	2019.03	254566.	225.76
10:06:12	3180.9	2019.03	256585.	225.81
10:06:37	3206.0	2023.06	258608.	225.86
10:07:02	3231.0	2018.22	260626.	225.92
10:07:27	3256.1	2023.06	262649.	225.96
10:07:52	3281.2	2019.03	264668.	226.01
10:08:17	3306.2	2019.03	266687.	226.06
10:08:42	3331.3	2018.22	268705.	226.11
10:09:07	3356.3	2019.03	270724.	226.15
10:09:32	3381.4	2018.22	272742.	226.21
10:09:57	3406.4	2015.00	274757.	226.27
10:10:22	3431.4	2018.22	276776.	226.31
10:10:47	3456.5	2019.03	278795.	226.37
10:11:12	3481.5	2018.22	280813.	226.42
10:11:37	3506.5	2019.03	282832.	226.47
10:12:02	3531.6	2019.03	284851.	226.52
10:12:27	3556.6	2018.22	286869.	226.58
10:12:53	3581.7	2019.03	288888.	226.63
10:13:18	3606.7	2018.22	290906.	226.68
10:13:43	3631.8	2023.06	292929.	226.73
10:14:08	3656.8	2015.00	294944.	226.79
10:14:33	3681.9	2018.22	296963.	226.84
10:14:58	3706.9	2019.03	298982.	226.89
10:15:23	3732.0	2018.22	301000.	226.95
10:15:48	3757.0	2019.03	303019.	227.01
10:16:13	3782.1	2019.03	305038.	227.05
10:16:38	3807.1	2018.22	307056.	227.11
10:17:03	3832.1	2019.03	309075.	227.15
10:17:28	3857.2	2018.22	311094.	227.21

10:17:53	3882.2	2019.03	313113.	227.25
10:18:18	3907.3	2023.06	315136.	227.31
10:18:43	3932.4	2019.03	317155.	227.37
10:19:08	3957.5	2023.06	319178.	227.42
10:19:33	3982.5	2018.22	321196.	227.47
10:19:58	4007.6	2019.03	323215.	227.52
10:20:23	4032.7	2023.06	325238.	227.57
10:20:49	4057.7	2019.03	327257.	227.61
10:21:14	4082.8	2018.22	329275.	227.66
10:21:39	4107.8	2019.03	331294.	227.71
10:22:04	4132.9	2018.22	333313.	227.75
10:22:29	4157.9	2015.00	335328.	227.79
10:22:54	4182.9	2018.22	337346.	227.85
10:23:19	4208.0	2019.03	339365.	227.90
10:23:44	4233.0	2018.22	341383.	227.94
10:24:09	4258.0	2019.03	343402.	227.98
10:24:34	4283.1	2019.03	345421.	228.02
10:24:59	4308.1	2018.22	347439.	228.07
10:25:24	4333.2	2019.03	349458.	228.12
10:25:49	4358.3	2023.06	351481.	228.16
10:26:14	4383.4	2023.06	353504.	228.21
10:26:39	4408.5	2023.06	355527.	228.25
10:27:04	4433.5	2019.03	357547.	228.29
10:27:29	4458.6	2018.22	359565.	228.34
10:27:54	4483.6	2019.03	361584.	228.37
10:28:19	4508.7	2018.22	363602.	228.42
10:28:44	4533.7	2015.00	365617.	228.46
10:29:10	4558.7	2018.22	367635.	228.49
10:29:35	4583.8	2019.03	369654.	228.52
10:30:00	4608.8	2018.22	371672.	228.56
10:30:25	4633.8	2015.00	373687.	228.61
10:30:50	4658.8	2018.22	375706.	228.64
10:31:15	4683.9	2019.03	377725.	228.69
10:31:40	4708.9	2018.22	379743.	228.72
10:32:05	4734.0	2019.03	381762.	228.76
10:32:30	4759.1	2023.06	383785.	228.80
10:32:55	4784.2	2023.06	385808.	228.83
10:33:20	4809.2	2019.03	387827.	228.86
10:33:45	4834.3	2018.22	389845.	228.89
10:34:10	4859.3	2019.03	391864.	228.94
10:34:35	4884.4	2019.03	393883.	228.96
10:35:00	4909.4	2018.22	395902.	229.01
10:35:25	4934.5	2019.03	397921.	229.03

10:35:50	4959.5	2018.22	399939.	229.06
10:36:15	4984.5	2019.03	401958.	229.10
10:36:40	5009.6	2019.03	403977.	229.14
10:37:05	5034.6	2018.22	405995.	229.17
10:37:30	5059.7	2019.03	408014.	229.19
10:37:56	5084.7	2018.22	410032.	229.23
10:38:21	5109.8	2019.03	412051.	229.26
10:38:46	5134.8	2019.03	414070.	229.28
10:39:11	5159.9	2018.22	416089.	229.31
10:39:36	5184.9	2019.03	418108.	229.34
10:40:01	5210.0	2018.22	420126.	229.37
10:40:26	5235.0	2019.03	422145.	229.40
10:40:51	5260.0	2019.03	424164.	229.43
10:41:16	5285.1	2018.22	426182.	229.46
10:41:41	5310.1	2019.03	428201.	229.49
10:42:06	5335.2	2018.22	430220.	229.51
10:42:31	5360.2	2019.03	432239.	229.54
10:42:56	5385.3	2023.06	434262.	229.56
10:43:21	5410.4	2019.03	436281.	229.59
10:43:46	5435.4	2018.22	438299.	229.61
10:44:11	5460.5	2019.03	440318.	229.64
10:44:36	5485.5	2018.22	442336.	229.66
10:45:01	5510.5	2015.00	444351.	229.69
10:45:26	5535.5	2018.22	446369.	229.70
10:45:51	5560.6	2019.03	448388.	229.72
10:46:16	5585.6	2018.22	450407.	229.75
10:46:42	5610.7	2019.03	452426.	229.77
10:47:07	5635.7	2019.03	454445.	229.80
10:47:32	5660.8	2018.22	456463.	229.82
10:47:57	5685.8	2019.03	458482.	229.85
10:48:22	5710.9	2018.22	460500.	229.87
10:48:47	5735.9	2019.03	462519.	229.88
10:49:12	5761.0	2019.03	464538.	229.90
10:49:37	5786.0	2018.22	466556.	229.94
10:50:02	5811.1	2023.06	468579.	229.94
10:50:27	5836.2	2019.03	470598.	229.96
10:50:52	5861.2	2019.03	472618.	229.98
10:51:17	5886.3	2018.22	474636.	229.99
10:51:42	5911.3	2019.03	476655.	230.02
10:52:07	5936.4	2023.06	478678.	230.04
10:52:32	5961.5	2023.06	480701.	230.05
10:52:57	5986.6	2023.06	482724.	230.07
10:53:22	6011.6	2019.03	484743.	230.10

10:53:48	6036.7	2018.22	486761.	230.11
10:54:13	6061.7	2019.03	488780.	230.14
10:54:38	6086.8	2018.22	490798.	230.14
10:55:03	6111.8	2015.00	492813.	230.16
10:55:28	6136.8	2018.22	494832.	230.17
10:55:53	6161.9	2019.03	496851.	230.18
10:56:18	6186.9	2018.22	498869.	230.20
10:56:43	6212.0	2019.03	500888.	230.37

ENL

11-86

DTIC